

## Preliminary Technical design for the SPIRAL 2 instrumentation

TITLE of the Project :

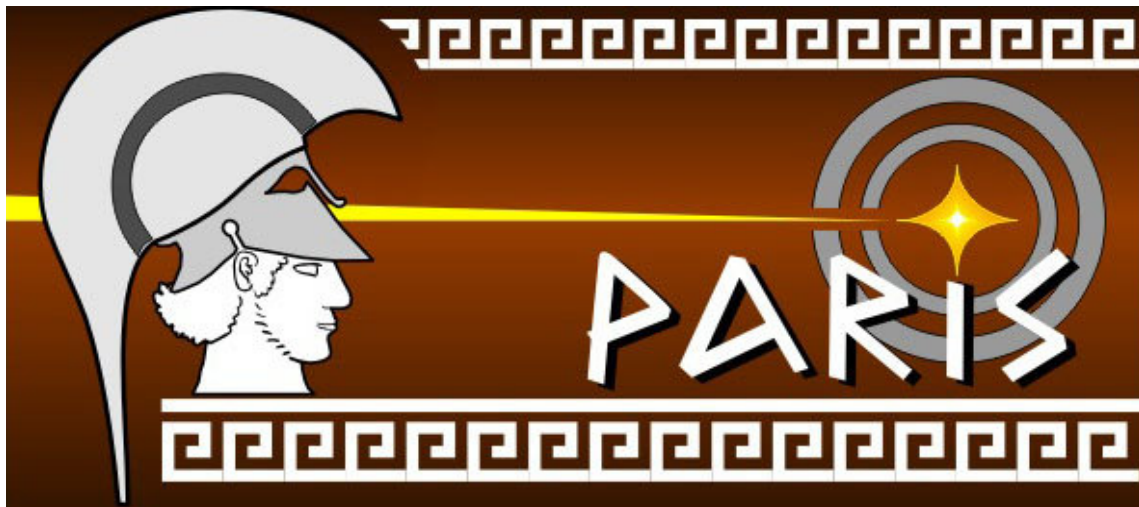
### **PARIS: Photon Array for studies with Radioactive Ion and Stable beams**

Abstract (Max 15 lines) :

*Note: This document **is not** the Technical Design proposal, as the PARIS project is not ready at this stage to prepare it. It is rather a detailed status report written using the Technical Design template, containing many alternative and preliminary scenarios. It will take about 1 year to be ready by the PARIS collaboration to prepare the real Technical Proposal.*

Fusion-evaporation reactions induced by high intensity neutron-rich beams from SPIRAL2 will allow us to populate exotic compound nuclei, transferring much more initial angular momentum to them than currently achievable with stable beams. This will be of great benefit for the study of vibrational and rotational collective phenomena at finite temperature, such as the Giant Dipole Resonance, exotic shape changes induced by fast rotation and structure of the very exotic nuclei. Heavy-ion radiative capture and reaction dynamics studies will also benefit considerably from the availability of high intensity neutron-rich beams.

Gamma ray detection constitutes an important experimental probe common to all these physics topics. Therefore the main aim of the PARIS collaboration is develop and to construct a dedicated gamma-calorimeter with dynamical range from 100 keV to 50 MeV, with the good energy resolution and with very good timing. Such a device might partly consist of existing European detectors. To complement the exciting challenges and opportunities afforded by SPIRAL2, it is also the intention to investigate designs for a novel gamma-calorimeter benefiting from recent advances in scintillator technology.



**Spokespersons** (maximum 3) with one corresponding spokesperson :

Name, Institution, E-mail address, Telephone number

Adam Maj, IFJ PAN Kraków (Poland), [Adam.Maj@ifj.edu.pl](mailto:Adam.Maj@ifj.edu.pl), +4812 6628 141

David Jenkins, University of York (UK), [dj4@york.ac.uk](mailto:dj4@york.ac.uk)

Jean-Antoine Scarpaci, IPN Orsay (France), [scarpaci@ipno.in2p3.fr](mailto:scarpaci@ipno.in2p3.fr)

**Contact person at GANIL :**

Jean-Pierre Wieleczko, GANIL (France), [wieleczko@ganil.fr](mailto:wieleczko@ganil.fr)

**Members of the Collaboration :**

Give the list of participating institutions and names of collaborators.

*IFJ PAN Kraków (Poland):* P. Bednarczyk, M. Kmiecik, B. Fornal, J. Grębosz, A. Maj, W. Męczyński, K. Mazurek, S. Myalski, J. Styczeń, M. Ziębliński, M. Ciemała, A. Czermak, R. Wolski, M. Chełstowska

*IPN Orsay (France):* F. Azaiez, J.A. Scarpaci, S. Franchoo, I. Stefan, I. Matea

*CSNSM Orsay (France):* G. Georgiev, R. Lozeva

*University of York (UK):* D.G. Jenkins, M.A. Bentley, B.R. Fulton, R. Wadsworth, O. Roberts

*University of Edinburgh (UK):* D. Watts

*IPN Lyon (France):* Ch. Schmitt, O. Stezowski, N. Redon

*IPHC Strasbourg (France):* O. Dorvaux, S. Courtin, C. Beck, D. Curien, B. Gall, F. Haas, D. Lebhertz, M. Rousseau, M.-D. Salsac, L. Stuttgé, J. Dudek

*GANIL Caen (France):* J.P. Wieleczko, S. Grevy, A. Chbihi, G. Verde, J. Frankland, M. Ploszajczak, A. Navin, G. De France, M. Lewitowicz

*LPC-ENSI Caen (France):* O. Lopez, E. Vient

*Warsaw University (Poland):* M. Kicinska-Habior, J. Srebrny, M. Palacz, P. Napiorkowski

*IPJ Swierk, Otwock (Poland):* M. Moszynski

*BARC Mumbai (India):* D.R. Chakrabarty, V.M. Datar, S. Kumar, E.T. Mirgule, A. Mitra, P.C. Rout

*TIFR Mumbai (India):* I. Mazumdar, V. Nanal, R.G. Pillay, G. Anil Kumar

*University of Delhi, New Delhi (India):* S.K. Mandal

*University of Surrey, Guildford (UK):* Z. Podolyak, P.R. Regan, S. Pietri, P. Stevenson

*GSI Darmstadt (Germany):* M. Górska, J. Gerl

*University of Oslo (Norway):* S. Siem

*Oak Ridge (US):* N. Schunck

*ATOMKI Debrecen (Hungary):* Z. Dombradi, D. Sohler, A. Krasznahorkay, G. Kalinka, J.Gal, J. Molnar

*INRNE, Bulgarian Academy of Sciences, Sofia (Bulgaria):* D. Balabanski,

*University of Sofia (Bulgaria):* S. Lalkovski, K. Gladnishi, P. Detistov

*NBI Copenhagen (Denmark):* B. Herskind, G. Sletten

*UMCS Lublin (Poland):* K. Pomorski

*HMI Berlin (Germany):* H.J. Krappe

*LBNL, Berkeley, CA (US):* M.-A. Deleplanque, F. Stephens, I.-Y. Lee, P. Fallon

*iThemba LABS (RSA):* R. Bark, P. Papka, J. Lawrie

*DSM/Dapnia CEA Saclay (France):* C. Simenel

*INFN-LNS, Catania (Italy):* D. Santonocito

*INP, NCSR "Demokritos", Athens (Greece):* S. Harissopoulos, A. Lagoyannis, T. Konstantinopoulos

*Istanbul University, Instambul (Turkey):* M.N. Erduran, M.Bostan, A. Tutay, M. Yalcinkaya, I. Yigitoglu, E. Ince, E. Sahin

*Nigde University, Nigde (Turkey):* S. Erturk

*Erciyes University, Kayseri (Turkey):* I. Boztosun

*Ankara University, Ankara (Turkey):* A. Ataç-Nyberg

*Kocaeli University, Kocaeli (Turkey):* T. Güray

*Flerov Laboratory of Nuclear Reactions, JINR, Dubna (Russia):* A. Fomichev, S. Krupko, V. Gorshkov.

*Uppsala University, Uppsala (Sweden):* H. Mach

*KVI, Groningen (The Netherlands):* M. Harakeh

*INFN Milano (Italy):* S. Brambilla, F. Camera, S. Leoni, O. Wieland.

*LPSC Grenoble (France):* G. Simpson

*INFN Napoli (Italy):* D. Pierroutsakou

*STFC Daresbury (UK):* J. Simpson, J. Strachan, M. Labiche

*Nuclear Physics Group, The University of Manchester (UK):* A. Smith

*RIKEN Tokyo (JP):* P. Doornenbal

## Table of contents

### 1. Introduction and Overview (max. 5 pages)

*Describe the main goal of the collaboration, the physics cases and the key experiments.*

## 1. Introduction and Overview

Nuclear reactions induced by beams of exceptionally high intensity as will be available in near future at GANIL will allow pushing further the limits of our understanding of the atomic nucleus, and address in detail longstanding vivid controversies. Exotic compound nuclei under extreme conditions of excitation energy and/or angular momentum can be reached by means of fusion reactions involving neutron-rich SPIRAL2 beams. The variety of the latter will offer the possibility of controlling the initial conditions in terms of nuclear composition and states to be populated. The study of single-particle and collective phenomena and their evolution with temperature and rotation, as well as nuclear dynamics from the astrophysical up to the multi-fragmentation energy domain are expected to benefit considerably from such a facility as developed in the PARIS Letter of Intent. As far as very intense stable LINAG beams are concerned, they will permit populating particularly neutron-rich nuclei either in one- and two-step fragmentation scenarios or via deep-inelastic and transfer mechanisms. That will allow investigating accurately nuclear structure at the drip-line, yielding strong constraints on the evolution of the interactions that govern the nuclear medium far from stability. The characteristics in energy, multiplicity and angular distribution of the  $\gamma$ -rays de-exciting the produced excited specie constitute a sensitive probe for all these physics topics. Yet, the specificities of the future beams imply quite un-usual working conditions, requiring namely the extraction of tiny cross sections within so far un-experienced large (radioactive) background and high counting rates. To succeed in the ambitious physics program, detection systems of new generation are mandatory. The PARIS collaboration, founded a couple of years ago, aims at building an innovative  $\gamma$ -array, playing the role of both an energy-spin spectrometer and a calorimeter for high-energy photons. The device is planned to be made of two layers based on most advanced scintillator technology for the inner volume - offering simultaneously high efficiency and relatively good energy resolution - and more conventional techniques for the outer part.

### 1.1. Physics Objectives

The PARIS project covers the interests and gathers the strengths of a wide range of the physics community. The programs to be conducted are briefly summarized in the following. In each case, the characteristics inherent to the  $\gamma$ -ray detection and required to bring to light a given physics point are emphasized. While most of the physics cases (\*) in the early Letter of Intent concentrate on heavy-ion collisions around the barrier, the beam energy domain of interest extended in the mean time according to the vivid interest manifested by several teams (\*\*) to join the collaboration. In addition, while the primary goal is to use PARIS at the SPIRAL2 facility, the installation of the array at the secondary target position of the  $S^3$  spectrometer - profiting from the future LINAG beams - is estimated as very promising as well.

#### *Jacobi shape transitions* \* (A. Maj, J. Dudek et al.)

The Jacobi shape transition corresponds to a nuclear shape change at high angular momenta from oblate to triaxial and very elongated prolate configurations. It has been predicted to appear in many nuclei in the liquid drop regime and is considered as a gateway to hyperdeformed shapes. The giant dipole resonance (GDR) line-shape is a very sensitive signature of this phenomenon: its strength function gets split according to the deformation of the system and a "giant back-bend" in the rotational frequency occurs at the highest spins. So far, firm evidence of a Jacobi transition has been found in light- and medium-mass nuclei only, and a preferential feeding of highly deformed structures by the GDR low-energy component has been observed in few cases. The difficulty of studying these phenomena in detail is for great part related to the narrow range in angular momentum  $L$  and excitation energy  $E^*$  it occurs in for light systems, and to the proximity of fission for heavy systems.

The GDR profile has therefore to be extracted properly and the multiplicity  $M_\gamma$  and energy sum  $\Sigma_\gamma$  of the statistical  $\gamma$ -rays has to be determined accurately, from which the  $(E^*, L)$  entry point is deduced.

***Shape phase diagrams of hot nuclei via the GDR differential method\**** (A. Maj, I. Mazumdar et al.)

Most nuclei are characterized by intrinsically deformed ground-state shapes caused by quantum shell effects. In the absence of rotation, thermal excitations wash shell effects out above a critical temperature and the equilibrium shape of the non-rotating nucleus is spherical. For a rotating system, one generally expects a non-collective oblate (i.e. rotating around the symmetry axis) configuration. However, theoretical calculations predict that many nuclei possess a temperature interval where rotation generates a prolate spheroid rotating along its symmetry axis (i.e. non-collective prolate) in contrast to that caused by the Jacobi transition. In such nuclei, a second critical temperature exists, above which the nucleus takes a non-collective oblate shape. These critical temperatures are spin- and most likely isospin-dependent. A tri-critical point in the  $(E^*, L)$  diagram - around which non-collective oblate, non-collective prolate, and collective tri-axial or oblate shapes coexist - is thus expected. Beside its line shape, the angular distribution of GDR  $\gamma$ -rays constitute a clear signature of the nature of the state. To explore such shape phase space transitions, the differential technique has shown very powerful: neighbouring compound nuclei are produced via different reactions in order to select a well-defined region in the  $(E^*, L)$  diagram. Yet, to fully exploit the technique, a particularly efficient and accurate multiplicity and energy sum filter is mandatory.

***Hot GDR studies in neutron-rich nuclei\**** (D.R. Chakrabarty, M. Kmiecik et al.)

In addition to its aforementioned shape dependence, the precise profile of the GDR, and namely its width, depends on temperature, angular momentum and presumably isospin. Fine structural effects and local shape transitions are difficult to unambiguously pinpoint experimentally, and further understand theoretically, if  $E^*$  and  $L$  remain un-controlled. To get insight into this puzzling interplay, the influence of temperature and spin have to be disentangled. That calls for a precise measure of the GDR profile and accurate  $M_\gamma$  and  $\Sigma_\gamma$  data. Once excitation energy and angular momentum effects are resolved, even more exotic phenomena such as the appearance of soft dipole modes towards more neutron rich systems can be reliably investigated.

***Isospin mixing at finite temperature\**** (M. Kicińska-Habior et al.)

The predicted trend of decreasing isospin mixing in  $N=Z$  nuclei at very high temperature has been confirmed experimentally by measuring the hindrance of E1 emission in  $T=0$  nuclei produced when two  $T=0, N=Z$  nuclei fuse. The GDR yield of the self-conjugate system is compared to that in a nearby  $N \neq Z$  nucleus, and the isospin mixing coefficient can be extracted using a statistical model. In contrast to the observed decreasing behaviour in light-mass nuclei, there are hints of an increasing isospin mixing coefficient going towards heavier systems. To investigate its magnitude and understand it in detail, more precise measurements on the GDR decay in medium- and heavy-mass nuclei with  $N=Z$  and nearby isotopes are necessary.

***Onset of multi-fragmentation and the GDR\**** (J.P. Wieleczko, D. Santonocito et al.)

The study of nuclei under extreme conditions, namely the question about the highest excitation energy a nucleus can sustain, is revealing of the transition from a semi-quantal low-energy regime - dominated by collective excitations and light-particle evaporation - to a statistical high-energy regime - with break up of the system into small pieces. When two ions collide, the compound system needs some time to equilibrate all its degrees of freedom. At very high energy, there is not enough time for developing a coherent collective behaviour such as a breathing, vibration or rotation. Correlations thus remain local and lead to the pre-formation of fragments inside the system. Repulsive Coulomb forces finally lead to a multi-fragmentation of the system. The development of "local sub-structures" implies the disappearance of the concept of the mean field. The GDR being a good indicator of the cohesion of an excited system, its disappearance and the saturation of its width, observed around 3-5MeV temperature depending on the mass, might be interpreted as a loss of collectivity and an evidence of a transition towards a chaotic regime. Nevertheless, the experimental information is very scarce and vividly debated. To unambiguously determine whether the potential saturation of the GDR width has to be linked to the on-set of a multi-fragmentation regime, observables typical for the low- and high-

energy regime have to be measured simultaneously over a wide range of temperature, and the width of the GDR profile has to be extracted with high accuracy, requiring high efficiency and good resolution.

***Reaction dynamics around the barrier and nuclear viscosity\**** (Ch. Schmitt, O. Dorvaux et al.)

The dynamical evolution of an excited compound nucleus as produced by a given entrance channel strongly depends on the viscous nature of nuclear matter. The latter implies a dissipation of energy between the collective and intrinsic degrees of freedom of the system. Due to the variety of shapes, excitation energies and angular momenta explored by the nucleus along its decay, no consensus emerges yet about the magnitude of this energy dissipation and its likely dependence on deformation,  $E^*$  and  $L$ . As a typical large-scale amplitude collective motion, fission stands for an excellent probe of nuclear viscosity. Of paramount interest is the time scale of the process, straightforwardly related to the underlying dynamics. Light-particles and GDR  $\gamma$ -rays have shown to establish pertinent clocks of fission time scales. Yet, both data set still disagree about the value extracted for the viscosity strength. To understand this discrepancy and exploit further these powerful tools, the predicted respective influence of temperature and angular momentum on dissipation phenomena has to be resolved first. To do so, the GDR decay has to be precisely sorted out according to excitation energy and spin i.e. it has to be measured in coincidence with  $\Sigma_\gamma$  and  $M_\gamma$ . Similarly, the GDR clock can be used to investigate the dynamics in the entrance channel, namely the competition between fusion and quasi-fission, which strongly hampers the synthesis of super heavy elements.

***Heavy-ion radiative capture\**** (S. Courtin, D.G. Jenkins et al.)

Heavy-ion radiative capture is a rare process due to the high Coulomb barriers and overwhelming competition from particle emission. Yet, unexpectedly large cross sections have been observed in some cases. They have been related to giant resonance enhancement of  $\gamma$ -ray decay widths, involving specific doorway states. A famous example is the radiative capture of  $^{12}\text{C}$  by  $^{12}\text{C}$ . The precise nature of the entry capture state could not be firmly determined yet. Nonetheless, the idea about doorways based on a molecular structure has been recognized as very valuable. These states seem to feed preferentially specific structures, namely highly deformed rotational bands in  $^{24}\text{Mg}$ . Usual statistical considerations involving many levels do therefore not hold any more; the system relaxes through a few specific states. Microscopic cluster approaches based on a many-body Hamiltonian and the Generator Coordinate Method have shown very pertinent in studying this phenomenon: They predict bands based on a  $^{12}\text{C}$ - $^{12}\text{C}$  “molecular” configuration which wave-function sizeably overlap with those of highly deformed states in  $^{24}\text{Mg}$ . To obtain more information about specific paths, both the energy and angular distribution of the highly energetic  $\gamma$ -rays that de-excite the corresponding states have to be measured with good resolution. In addition, to isolate properly the capture states, the measure of the energy sum is highly desirable.

***Multiple Coulex for Super-Deformed bands\*\**** (P. Napiórkowski, F. Azaiez, A. Maj et al.)

The electromagnetic properties of super-deformed (SD) bands in nuclei around  $^{40}\text{Ca}$  are proposed to be investigated by means of Coulomb excitation below the barrier. An accurate determination of the transition probabilities for both in- and out-of-band transitions is revealing of the underlying SD structure. A good resolution is required for single SD  $\gamma$ -rays in the [2-6]MeV range. Efficiency is of primary importance for tracking down the tiny population of the SD branch.

***Astrophysics\*\**** (S. Harissopulos et al.)

The accurate determination of the cross sections of capture reactions of astrophysical interest is very challenging due to the weak probability of the reaction channel and overwhelming background. A innovative technique - called  $4\pi$  summing method - has shown very powerful in this respect: The cross section is derived from the number of cascades between the entry capture state and the ground state, independently on the depopulation path. Basically the energy sum  $\Sigma_\gamma$  has to be determined with good resolution and the yield in the corresponding peak has to be measured with extremely high efficiency. Information on multiplicity  $M_\gamma$  is important for evaluating the efficiency, while angular distributions permit minimizing the background.

***Spectroscopy close to the neutron drip-line\*\**** (F. Azaiez, Z. Dombradi *et al.*)

The vanishing of the well-known magic numbers 2, 8, 20, 28, 50, ... far from stability towards the neutron drip-line and the existence of an island of inversion is still controversial. Nuclear level schemes are of primary importance for determining the existence of shell gaps and understanding the underlying single-particle structure.

- **Using reactions induced by in-flight radioactive nuclear beams at S<sup>3</sup>**

Neutron-rich species can be populated efficiently in multi-nucleon transfer and deep inelastic reactions taking profit from very intense LINAG stable beams in an in-flight mode using the S3 spectrometer and a high-power rotating target. Provided reasonable rates and energies above the barrier for the produced beams, a large variety of secondary reactions such as (in-)elastic scattering, transfer, deep-inelastic and fusion-evaporation reactions can be explored to form even more exotic nuclei which level scheme is still virgin. In the very near future, cross sections using one of this production method, namely deep-inelastic collisions close to 0°, will be measured and compared to model calculations. From that detailed investigation, the possibility of measuring the energy of the 2<sup>+</sup> state in <sup>78</sup>Ni and check the effectiveness of its double magicity will be evaluated. The study of the structure of neutron-rich nuclei produced this way calls for a very efficient device according to the small cross sections involved and the few states populated.

- **Via intermediate energy experiments**

Particularly neutron-rich light nuclei ( $A \sim 20$ ) are proposed to be produced by means of a two-step fragmentation scenario. To establish firmly the level scheme of the isotopes of interest, de-exciting  $\gamma$ -rays with energies in the [1-4]MeV range have to be measured in coincidence and with good resolution. According to the low secondary beam intensity involved, high efficiency is primordial.

***Relativistic Coulex\*\**** (P. Bednarczyk *et al.*)

The properties of the first 2<sup>+</sup> level in even-even exotic nuclei, such as excitation energy and reduced electric quadrupole transition probability B(E2), are essential for understanding fundamental nuclear structure phenomena as magic shell evolution, new shell closures, nuclear deformation and soft collective modes (E1 strength) far off the stability line. It is proposed to populate such states by means of Coulomb excitation involving relativistic beams. It has been shown that this method provides a selective tool to investigate low-lying excited states. The energy of single  $\gamma$ -rays has to be measured with good resolution. High efficiency is important as well due to the low cross sections.

This physics case requires use of fast beams, so it will be of relevance when using PARIS at FAIR, RIKEN or after upgrade of SPIRAL2 with post-accelerated radioactive beams.

***Nuclear Moments measurements\*\**** (G. Georgiev, D. Balabanski *et al.*)

Nuclear electromagnetic moments are known as very sensitive probes of the structure of the atomic nucleus. Magnetic dipole moments give detailed information on the wave-function and single-particle properties. Electric quadrupole moments provide direct information on the collective properties and the deformation of the nuclear state. Obviously, both single-particle and the collective properties are indispensable for discussing the development of “new” shell closures far from stability. The Time Dependent Perturbed Angular Distribution method has proven very powerful for nuclear moments measurements of isomeric states. It requires the detection of  $\gamma$ -rays as a function of angle and time, implying precise and wide angular coverage and fast timing, respectively. In addition, a multiplicity filter function permits performing prompt-delayed  $\gamma$ - $\gamma$  coincidences. That is very important when populating the isomeric states of interest by means of transfer reactions.

## 1.2. PARIS specifications

According to the large variety of subjects presented in the SPIRAL2 Letter of Intent, a ‘Physics Cases and Theory’ working group has been formed at the very beginning of the PARIS collaboration. It is intended to coherently highlight the fundamental physics issues to be addressed by the new device. In a first stage, the contacts established with the theoreticians involved in the Letter of Intent as well as with several others have been strengthened. This natural bridge between theory and experiment

permitted investigating how unambiguously evidencing a given phenomenon - keeping in mind the resolution realistically achievable in experiment. A summary of this work has been presented at the PARIS meeting held in Cracow in May 2007<sup>1</sup>. In a second stage, intense effort has been invested in finding the best compromise for enlarging the physics program to a few more exciting topics, implying in most cases different techniques. Special attention has been paid on the specific constraints inherent to the various subjects. The outcome of preliminary thoughts has been presented in May 2008 at the PARIS meeting in York<sup>1</sup>. By triggering discussions, a smooth synergy between respective goals and requests has emerged within the collaboration.

From the survey of the above-described physics cases, the most crucial requirements for the device to be constructed become clear. The energy resolution shall be of the order of (3-5)% up to photon energies around 40MeV. The desired accuracy of the entry point location in the ( $E^*$ ,  $L$ ) space demands a resolution of about 5% for the energy sum and below 4 for the  $\gamma$ -ray multiplicity. These numbers imply **high efficiency**, **wide angular coverage** and **sufficient granularity**. High efficiency is essential for all the physics cases due to low cross sections and/or overwhelming background. In the same line, the angular coverage should be as close as possible from  $4\pi$ . Together with granularity, this feature is even more important when angular distributions have to be measured. **Good timing properties** are crucial as well: The time-of-flight resolution has to match the sub-nanosecond level in order to remove unwanted background. Scintillator materials of new generation seem to cope with all these requirements. For  $\gamma$ -ray energies above about 2MeV, relatively low multiplicities and fast beams - as it is often the case for spectroscopy studies of exotic light neutron-rich nuclei, LaBr<sub>3</sub> scintillators compete with Ge detectors in terms of resolution while being more efficient, what is advantageous for low cross sections and/or beam intensities. Although not explicitly mentioned in the above, nearly all listed physics cases require ancillary detectors in addition to the PARIS array. These are namely (i) heavy-ion spectrometers for selecting the mechanism and in some cases fully identifying the reaction product as well as determining its velocity as suited for Doppler correction, (ii) light-particle detectors to reconstruct the kinematics of the process and sometimes (iii) high-resolution Ge detectors (e.g. EXOGAM2 or AGATA) to complement PARIS when pursuing discrete low-energy  $\gamma$ -rays. This mandatory coupling to various other instruments necessitates a **versatile device**.

A detailed list of requirements classified according to the physics case has been established and summed up in Table 1. This compilation constitutes a crucial input for the working groups dealing with simulations, electronics and mechanics. All together finally defines the specifications of PARIS. As the present report shows, these are currently under detailed study and - if still open - final decisions are coming to be taken in very near future.

---

<sup>1</sup> <http://paris.ifj.edu.pl>

Physics Case	Recoil mass	v/c [%]	$E_\gamma$ range [MeV]	$\Delta E_\gamma/E_\gamma$ [%]	$\Delta E_{\text{sum}}/E_{\text{sum}}$ [%]	$\Delta M_\gamma$	$\Omega$ coverage	$\Delta T$ [ns]	Ancillaries	Comments
Jacobi transition	40-150	<10	0.1-30	4	<5	4	$2\pi-4\pi$	<1	AGATA HI det.	High eff. Beam rej.
Shape Phase Diagram	160-180	<10	0.1-30	6	<5	4	$2\pi-4\pi$	<1	HI det.	High eff. Differential method Beam rej.
Hot GDR in n-rich nuclei	120-140	<11	0.1-30	6	<8	4	$2\pi-4\pi$	<1	HI det.	Beam re.
Isospin mixing	60-100	<7	5-30	6	-	-	$4\pi$	<1	HI det.	High eff. Beam rej.
Reaction dynamics	160-220	<7	0.1-25	6-8	<8	4	$2\pi$	<1	n-det. FF det.	Complex coupling
Collectivity vs. multi-fragmentation	120-200	<8	5-30	5	-	-	$2\pi$	<1	LCP det. HI det.	Complex coupling
Radiative capture	20-30	<3	1-30	<4	5	-	$4\pi$	<1	HI det.	High eff.
Multiple Coulex	40-60	<7	2-6	5	-	-	$2\pi$	<5	AGATA CD det.	Complex coupling
Astrophysics	16-90	0.1	0.1-6	6	5	-	$4\pi$	<1	Outer PARIS shell as active shield	High eff. Back-ground
Shell structure at intermediate energies (SISSI/LISE)	16-40	20-40	0.5-4	3	-	-	$3\pi$	<<1	SPEG or VAMOS	High eff. Low $I_{\text{beam}}$ $\gamma$ - $\gamma$ coinc
Shell structure at low energies (separator part of $S^3$ )	30-150	10-15	0.3-3	3	-	-	$3\pi$	<<1	Spectrometer part of $S^3$	High eff. Low $I_{\text{beam}}$ $\gamma$ - $\gamma$ coinc
Relativistic Coulex	40-60	50-60	1-4	4	-	1	Forward $3\pi$	<<1	AGATA HI analyzer	Ang. Distr. Lorentz boost
Nuclear Moments	30-15-	0	0.1 - 4	3	-	4	$3\pi - 4\pi$	<1	Permanent magnet, particle det.	Stopped ion

**Table 1:** List of requirements related to the different physics cases to be addressed at PARIS.

### 1.3. Towards key experiments

In close cooperation with the other working groups and following the latest progress of the ‘GEANT4 Simulations’ group, the ‘Physics Cases and Theory’ team investigates most relevant key experiments to be run at the different stages of the development of PARIS. Concrete propositions already emerged thanks to discussions during the collaboration meetings. As priority flagship experiments, two reactions dealing with the early physics cases of the Letter of Intent and one related to the new topics have been selected.

#### *Jacobi shape transition in light nuclei*

The goal is to study in more detail the evidence of a Jacobi transition in the light  $^{46}\text{Ti}$  nucleus. In addition, it has been found that the de-excitation of the  $^{46}\text{Ti}$  compound by a GDR  $\gamma$ -ray and an  $\alpha$  particle populates preferentially the SD band in  $^{42}\text{Ca}$ , which properties are interesting on their own. Jacobi transitions in light nuclei have the advantage of being characterized by well-separated and localized shapes as a function of angular momentum. Potential energy minima are stiff, barriers are high, deformations are large and fission is far away. Yet, the gradual shape transition occurs over a narrow range in  $L$ , necessitating an accurate spin spectrometer. A *test key experiment* could be already done using stable beams (e.g.  $^{18}\text{O}+^{28}\text{Si}$ ) and coupling the PARIS demonstrator with HECTOR and EXOGAM. While the former permits investigating PARIS performances both in terms of accurate spin spectrometer and efficient high-energy  $\gamma$ -ray calorimeter, the latter permits tagging precisely the SD band of  $^{42}\text{Ca}$ . Doppler effects are planned to be corrected by an upgrade of the RFD separator. A similar experiment used HECTOR, EUROBALL IV and EUCLIDES.

The difficulty inherent to the experimental study of these phenomena is related to the spin window covered by the oblate-triaxial Jacobi shape change and the proximity of the fission limit. Favourable conditions are expected to be met in exotic, neutron-rich nuclei, accessible via fusion-evaporation with the advent of SPIRAL2 beams. Therefore as the *real key experiment* on the Jacobi shape transition we consider the compound nucleus  $^{120}\text{Cd}$  which can be produced at very high angular momentum, almost reaching  $100 \hbar$ , in inverse kinematics by the SPIRAL2  $^{94}\text{Kr}$  beam impinging on  $^{26}\text{Mg}$ . This will require a coupling of the  $2\pi$  PARIS array to the AGATA Demonstrator and RFD.

### ***Heavy-ion radiative capture***

Radiative capture is proposed to be investigated in detail for the  $^{12}\text{C}+^{12}\text{C}$  test case. From the theoretical point of view, identical bosons in the entrance channel minimize complex aspects, while on the experimental side previous studies still had to face poor statistics and restricted sensitivity, precluding firm conclusions to be established. Since for such an experiment high efficiency and wide angular coverage are primordial, the full PARIS available at the time is required. In addition, to select properly the entry capture state and correct precisely for Doppler effects, a heavy-ion spectrometer is highly desirable.

### ***Nuclear spectroscopy at the neutron drip-line***

The PARIS array is proposed to be installed at the secondary target position of  $S^3$  for measuring in-beam gamma rays emitted from secondary reaction products with large neutron to proton excess. The  $S^3$  spectrometer will be used to select a given secondary beam, that further interacts in a second target leading to the very exotic specie of interest. PARIS detectors in conjunction with AGATA and EXOGAM2 detectors could be used to measure the spectroscopy of these exotic nuclei which are identified with the second half of  $S^3$ . This type of experiment will be certainly one of the first that will be performed with the high intensity stable ion beams from LINAG. Though, the present design of  $S^3$  does not foresee a large space around the mid-point of the spectrometer where PARIS and other detectors could be used.

## 2. Description of the proposed equipment(s)

### 2.1 Design specifications

#### **PARIS design goals:**

Design and build high efficiency detector consisting of 2 shells (ev. 1 shell + tracking) for medium resolution spectroscopy and calorimetry of gamma-rays in large energy range.

Inner (hemi-)sphere, highly granular, will be made of new crystals ( $\text{LaBr}_3(\text{Ce})$ ), rather short (up to 2-4 inches). The readout might be performed with PMTs or APDs. The inner-sphere will be used as a multiplicity filter of high resolution, sum-energy detector (calorimeter) and detector for the gamma-transition up 10 MeV with medium energy resolution (better than 3%). It will serve also for fast timing application.

Outer (hemi-)sphere, with lower granularity but with high volume detectors, rather long( at least 5 inches), could be made from conventional crystals ( $\text{BaF}_2$  or  $\text{CsI}$ ), or using existing detectors (Chateau de Crystal or HECTOR). The outer-sphere will measure high-energy photons or serve as an active shield for the inner one.

Array has to be mechanically compatible with AGATA or EXOGAM2 and possibly with other detectors, as for example GASPARD, Neutr. Det, INDRA/FAZIA.

### 2.2 Simulations

## **1. Introduction**

The aim of the PARIS collaboration is to design an array of  $\gamma$  detectors that can serve at the same time as a sum-spin spectrometer and a calorimeter for high-energy  $\gamma$ -rays, possessing also good energy and

time resolution. The most widely used scintillators for such arrays have been the Na(Tl), BGO, CsI and BaF<sub>2</sub> crystals. The recently developed LaBr<sub>3</sub>:Ce scintillator provides excellent intrinsic characteristics that can potentially strongly improve the current devices.

- The high Z and high density allow an efficient detection over a large range of energies. Fig 1. shows the full absorption probability, based on a 20 cm thick full shell, for the new material and the most commonly used. Except for BGO, it appears clearly that LaBr<sub>3</sub> provides the best absorption cross section.
- Unlike BGO, LaBr<sub>3</sub> achieves an excellent energy resolution of about 3% at 662 keV. In addition the fast timing allows considering neutron- $\gamma$  separation by time-of-flight even at distances relatively closed to the target position.

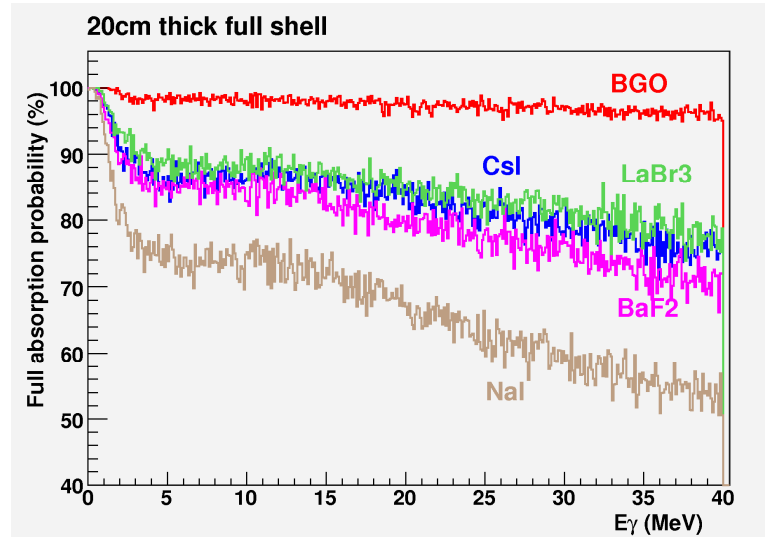


*Fig. 1: Full absorption probability for full shells (20cm radius) made of different scintillators*

The full array should be designed to take advantages of the excellent intrinsic characteristics without deteriorating them.

Considering the photo peak efficiency, the device should cover as much as possible  $4\pi$ . The crystal depth impacts directly on the full absorption probability. Because such new material is very expensive, one may not be able to build a device as deep as it should be required by the different physics cases to be addressed, in particular for high energy  $\gamma$ -rays up to 50 MeV. An original proposition is to have two layers of scintillators, the first one being composed of LaBr<sub>3</sub>, the second one of another less expensive material. In such a case, the first shell is used as a sum-spin spectrometer while the second one is devoted to high-energy  $\gamma$ -rays. One of the crucial question to be addressed by realistic simulations is to prove that building such a device has a sense. Indeed, the first layer is likely to absorb also high-energy  $\gamma$ -rays.

Of course, one may also consider to have enough money (and the technology) to build an array composed of only one layer of LaBr<sub>3</sub>. In such case, there is no more information from the in-depth segmentation due to the two layers. This information may be important to disentangle the different kind of events detected and could be thus used in the reconstruction algorithms applied.

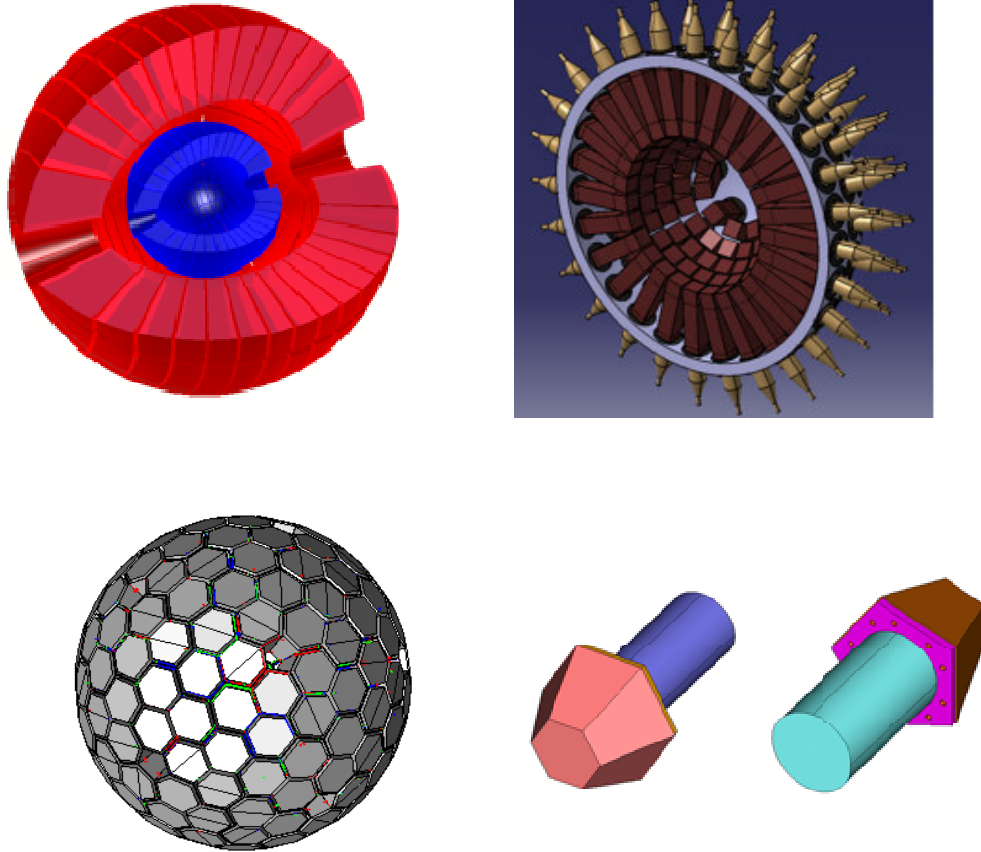


*Fig. 2: Different geometries belonging to the first family of configurations*

Considering the excellent energy resolution, it is crucial to not spoil it. For that, the Doppler broadening should be kept as small as possible (less than 3%) for the physics cases to be addressed: it implies a consequent segmentation. Increasing the segmentation has also the advantage to reduce pile up effects which enable to obtain the multiplicity of a  $\gamma$ -ray cascade with less errors. The price to pay for highly segmented devices is the complexity of the algorithms used to reconstruct properly the different kind of events.

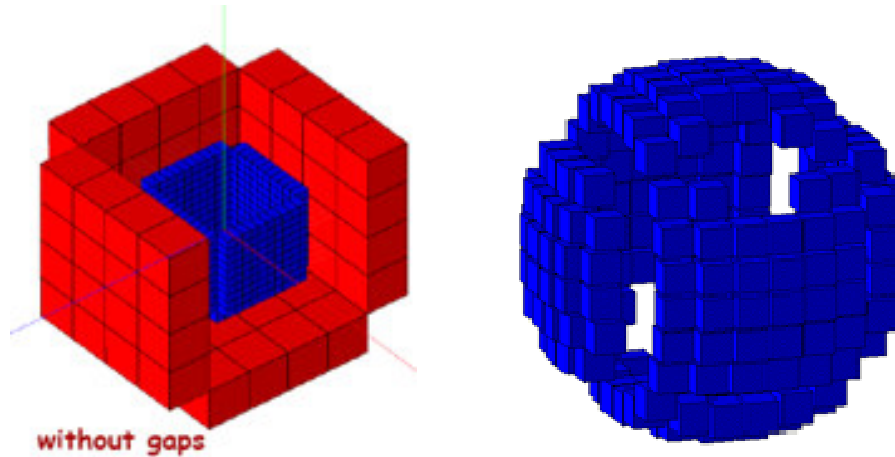


*Fig. 3: Two geometries belonging to the second family of configurations*

In order to bring some answers to the previous mentioned questions, a GEANT4 package has been developed and has been used to study different configurations. An ‘ideal’ geometry, composed of one or two concentric spheres has helped to establish the best allowed performances. It is as well a perfect benchmark to understand how the various  $\gamma$ -rays are absorbed and it gives then precious information for the reconstruction algorithms. A virtual segmentation is applied at the analysis level allowing to study this aspect quite easily.

More realistic geometries have been investigated based on current available LaBr<sub>3</sub> crystal shapes (rectangle of dimensions 2”x2”x2”, 1”x1”x4” or 2”x2”x4”) or more exotic ones (pentagon and hexagon) that may be produced in the future. Except for the fact that arrays with one or two layers have been studied, the proposed geometries could be grouped in two families: the first one corresponds to an isotropic arrangement while the second one is based on a less-isotropic arrangement i.e. on a ‘cubic-like’ configuration. In Figure 2 are displayed some geometries belonging to the first family. The top left panel shows the ‘ideal’ case composed of two full concentric spheres with a virtual segmentation applied at the analysis level. A half sphere array made of 100 phoswiches elements is represented in the top right panel (the full device is composed of two half spheres, 200 elements). In this case, the two layers are stacked together (LaBr<sub>3</sub> and CsI) and the basic elements have a rectangular shape: it is referred as the ‘wheel’ configuration.

Configurations based on pentagonal and hexagonal crystal shapes (see bottom right panel) have also been simulated (referred as a ‘soccer ball’ configuration), one with a relatively small number of elements (about 30), one with a higher number (AGATA-like geometry with 180 elements, see bottom left panel), both composed of only one layer.

Current LaBr<sub>3</sub> crystals are made with a rectangular shape. One could then easily build a full array keeping such geometry as shown in Fig. 3 where two configurations illustrating the second family are given. On the right panel the elements (only the first layer represented) are shifted so that it mimics a sphere like configuration. Other propositions could be considered (barrel-like approach with end caps) in the future to have a configuration that fully exploit the excellent intrinsic characteristics of the LaBr<sub>3</sub> material.

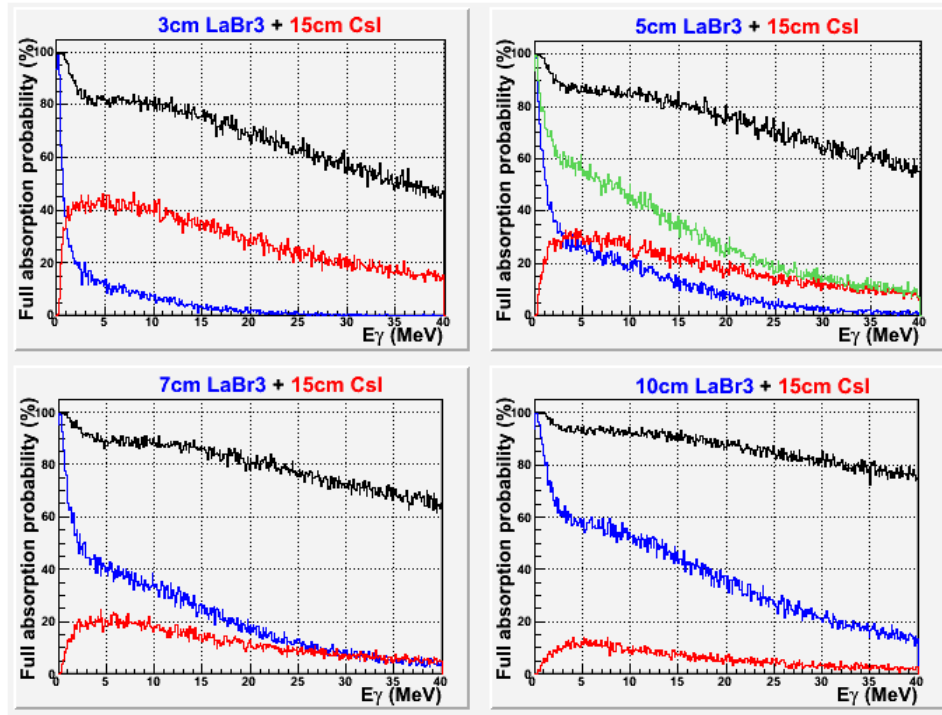


*Fig. 4: Full absorption efficiency for different ‘ideal’ configurations.*

## 2. Full absorption efficiency

In this section are given the main results concerning the full absorption efficiency for the different configurations so far under considerations. The studies are done by shooting, from the centre of the array, a single  $\gamma$ -ray (multiplicity one) with various energies. Figure 4 gives the best expected characteristics for the full array and allows to explain how  $\gamma$ -rays interact with the detector. These results have been obtained with the ‘ideal’ configuration composed of two full concentric spheres. The first one is made of LaBr3 with a depth that grows from 3cm to 10cm. The second layer is made of CsI with a fixed depth (15cm). The plot represent the full absorption probability for the first shell (in blue), the second one (in red) and for the whole array (in black). As expected, the photo peak efficiency increases in the first layer as the depth becomes greater. It reaches respectively 54% and 80% (at 1MeV) for 5cm and 10cm of LaBr3. It should be notified that these numbers have been obtained by applying a full addback procedure which could be done only at multiplicity one. In the top right panel is also given, for the corresponding configuration, the histogram (in green) obtained by summing the full absorption probability of the first layer (blue) to the second one (red). As it can be seen, the green curve is still far from the black one showing that a great number of high energy  $\gamma$ -ray deposits their energy in the two shells: an efficient addback procedure between the two layers would increase consequently the full absorption especially at the highest energies.

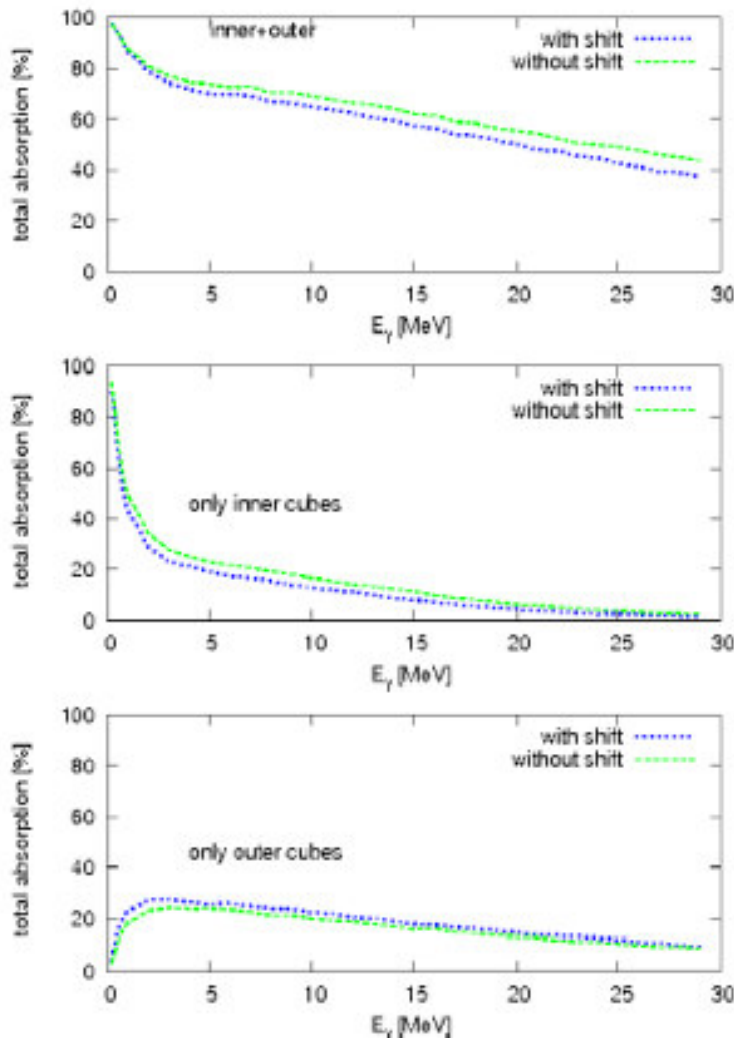


*Fig. 5: Full absorption efficiency for a 'pure cubic' arrangement and a shifted one.*

Going into details, the photo peak process dominates at very low energy and  $\gamma$ -rays are fully absorbed in the first shell. Then, the Compton diffusion becomes the main process up to about 6 MeV. The cross section decreases with the energy and thus the first layer is more and more transparent. In the pair creation regime, the mean free path decrease with the energy : the first layer becomes more and more opaque. While the first interaction point is likely to be in the first layer, the second one is required to fully absorbed the electromagnetic shower which is longer and longer. Note that the addback between the two layers could be considered, however we should keep in mind that the intrinsic resolution of the second one may not be as good as the first one. For that class of events, the good intrinsic resolution of LaBr<sub>3</sub> would then be spoiled.

Building a compact sphere using rectangular shapes is problematic as it is illustrated in fig. 3 (top right panel) in which 200 phoswiches (LaBr<sub>3</sub>+CsI) modules have been placed around the target. The solid angle covers by LaBr<sub>3</sub> is reduced (8.26 sr) and the distance between two modules increases as the radius increases. For the inner layer, the photo peak efficiency drops to 25 % while 54 % are expected from the 'ideal' case. The factor for the outer layer is even much more important (reduction by a factor about 10 at 10 MeV). Because this layer is made of more common materials, one may use more

adapted shapes which could cover more space and gives then a much better detection efficiency for high-energy  $\gamma$ -rays. One could also supposed that new shapes (pentagonal, hexagonal) would be available for LaBr3 crystals in the future. To check what could be lost due to spacing between modules and dead materials, simulations have been performed based on a "soccer ball" configuration. The lost in photo peak efficiency is less important with respectively 5% and 10% less for 1MeV and 15 MeV (considering only one layer of LaBr3).

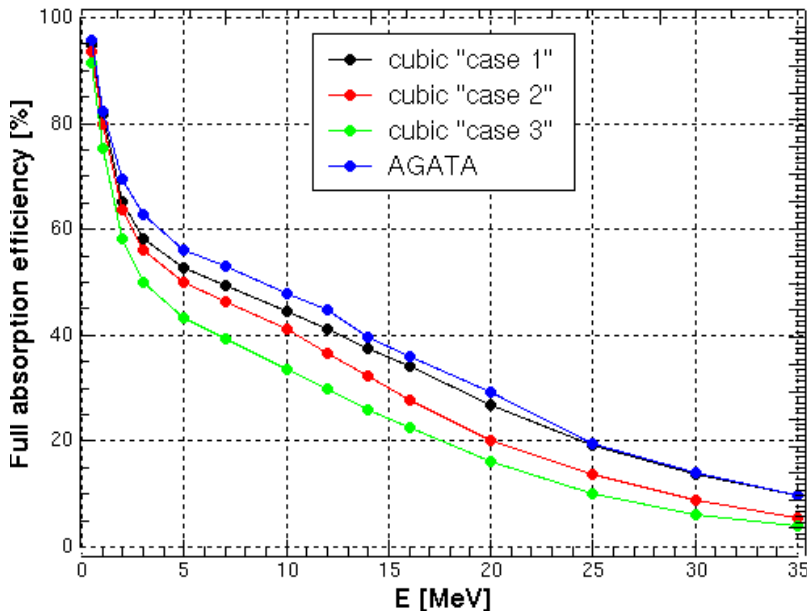
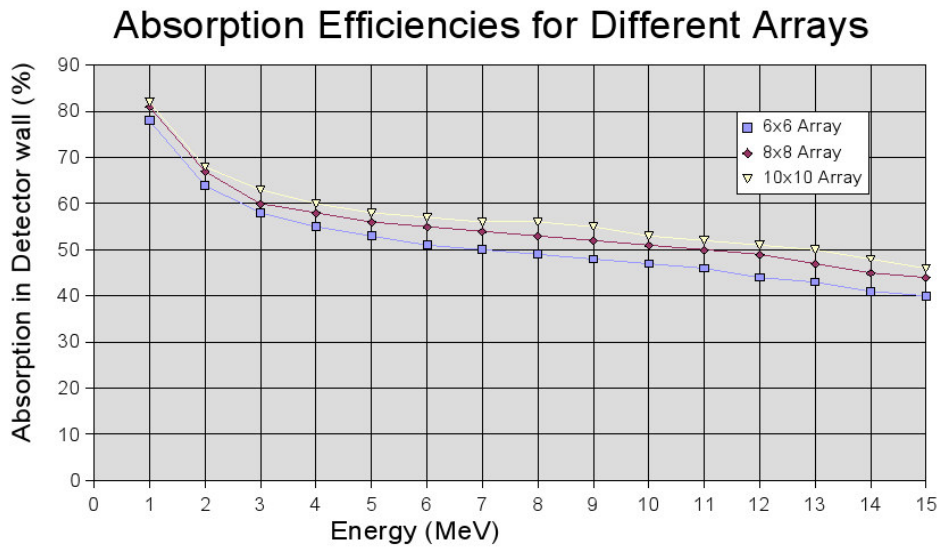


Fig. 6: Full absorption efficiency for the Agata-like configuration and a 'cubic-like' arrangement

Geometries based on a cubic configuration allow more compact arrangements as shown in Fig. 3. A disadvantage is a non-negligible dependence of the efficiency as function of the emission angle. Photo peak efficiency have been established for a pure 'cubic-like' arrangement and an 'ideal' configuration under similar conditions (the depth of the material used for the two layers). The lost in the full absorption probability are of the same order that for the 'soccer ball' configuration i.e. about 5% at 1 MeV and 13 % at 10 MeV (but in this case without spacing between the crystals and without dead materials). Shifting a little bit the cubes to mimic a sphere (see Fig 3) implies an additional lost of the photopeak efficiency, especially at high energy, as it is shown in Fig. 5. While the differences between the 'cubic' and the 'ideal' configuration may come from the lack of matters in the corners of the former, the differences with the shifted one indicate  $\gamma$ -rays are less efficiently absorbed in such anisotropic configurations. This is illustrated by the next study (Fig 6) that compares the full absorption efficiency for a shifted cubic configuration with the AGATA-like one (based on 180 crystals) which is one of the most compact geometry based on hexagonal shapes. The three cases for the 'cubic' arrangement refer to different conditions for the simulation. A narrow beam of  $\gamma$ -rays has been shot in three well defined directions (5.57, 17.73 and 28.59 degrees).

While the depth of an AGATA crystal is 9cm, the simulations have been done with 2"x2"x4" LaBr3 crystals for the shifted array i.e. equivalently 10cm for the depth. Despite the additional quantity of materials, the photo peak efficiency is lower by a factor 3% to 20% depending of the  $\gamma$ -ray energy. It also depends significantly of the emission angle.

For this 'cubic-shifted' configuration, one may increase the efficiency by adding more crystals. This is illustrated in Fig. 7 where is given the full absorption efficiency for different arrangements: 6x6, 8x8 and 10x10 elements per faces of the cube. Of course, the distance from the target increases by adding elements (1"x1"x4" crystals) from 15.24 cm (6x6 configuration) to 25.4 cm (10x10 configuration).



*Fig. 7: Gain in full absorption efficiency in a 'cubic' configuration by increasing the number of modules in the array*

### 3. Segmentation and reconstruction

The response function has been extensively studied at multiplicity one for several different configurations. In the following section, the segmentation of the array is discussed and the first studies on reconstruction algorithms are presented.

The Doppler broadening is the main effect that can spoil the good intrinsic resolution of LaBr<sub>3</sub> crystals. At first order, it is proportional to the recoil velocity and to the opening angle of the crystal. Studies have shown, for a reasonable range of recoil velocities (up to 30%), that the opening angle should be less than 20 degrees to have an additional error on the energy resolution of the same order that the intrinsic one (about 3%). With a smaller value (6 degrees), the contribution of the Doppler broadening would be negligible. In case the device should be adapted for higher recoil velocities, the concept of a symmetric configuration should be given up to take into account the Lorentz boost. A minimum of nine rings is then required to keep the Doppler broadening reasonable for the various physics

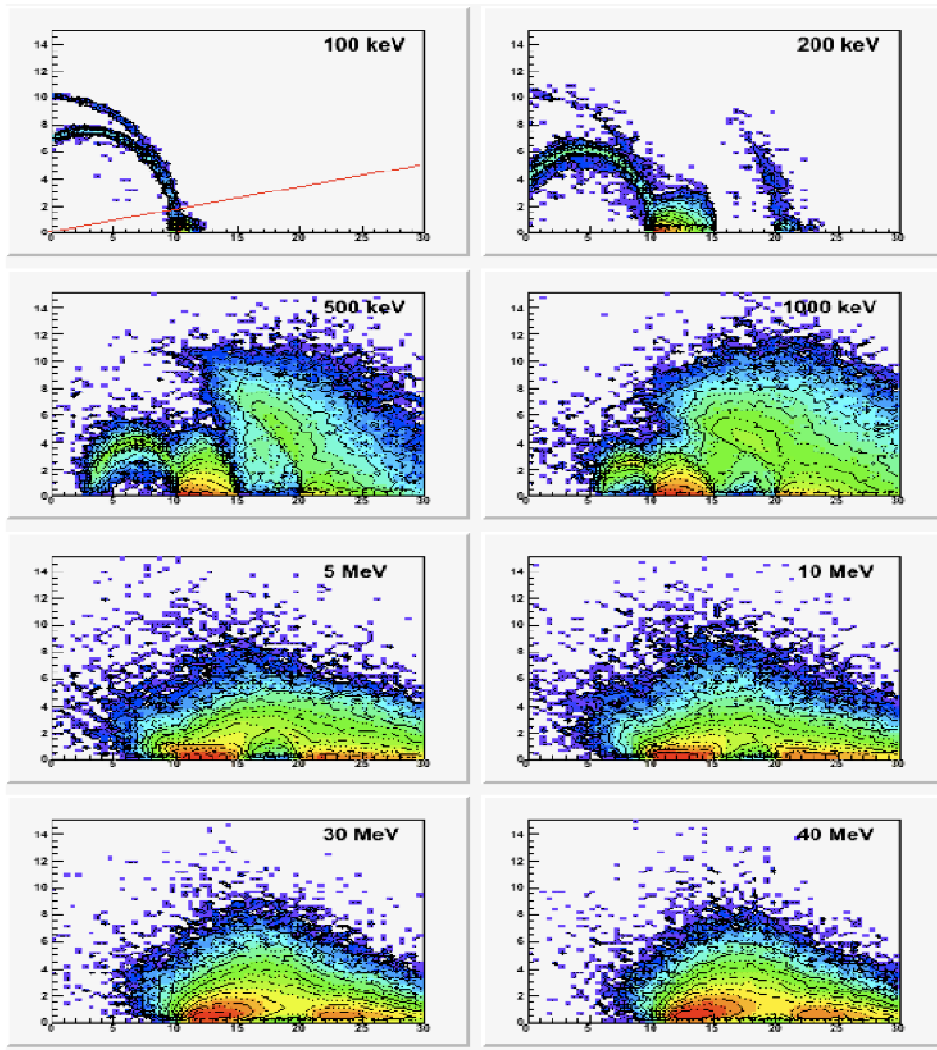


*Fig. 8: Illustration of how  $\gamma$  rays are absorbed in an 'ideal' configuration*

cases to be addressed by PARIS. This could be achieved with 2"x2" crystals at a minimal distance of 15cm.

As a sum-spin spectrometer, PARIS should have also a segmentation large enough to keep the pile up effect as low as possible. It does not affect strongly the resolution on the energy part but impacts more consequently on the multiplicity determination. For a cascade of 30  $\gamma$ -rays, to keep a pile up probability less than 10%, a crude estimation requires an opening angle not greater than 7.2 degrees. This estimation does not include neither the energy dependence of the  $\gamma$ -ray nor the real geometry of the setup.

To keep the good intrinsic resolution of the LaBr3 scintillators, one should also avoid a too large segmentation which would imply to addback too much segments to reconstruct the  $\gamma$ -ray energy. The 'ideal' geometry has been used to explore how an incident  $\gamma$ -ray is absorbed in the array for the different regimes: photopeak, Compton scattering and pair creation. This is illustrated in fig. 8 for which a configuration of two concentric spheres have been used. The first one is made of LaBr3 (radius from 10cm to 15cm) and the second one of CsI (radius from 20cm to 35cm). The picture gives the mean position where the energy is deposited in the array for various  $\gamma$ -ray shot horizontally. In the first panel is shown in red an opening angle of 10 degrees. Even if the energy may be spread around, it

can be seen the majority of the events deposit their energy within a cone delimited by 10 degrees. Consequently, the addback procedure should be applied with the closest neighbours.

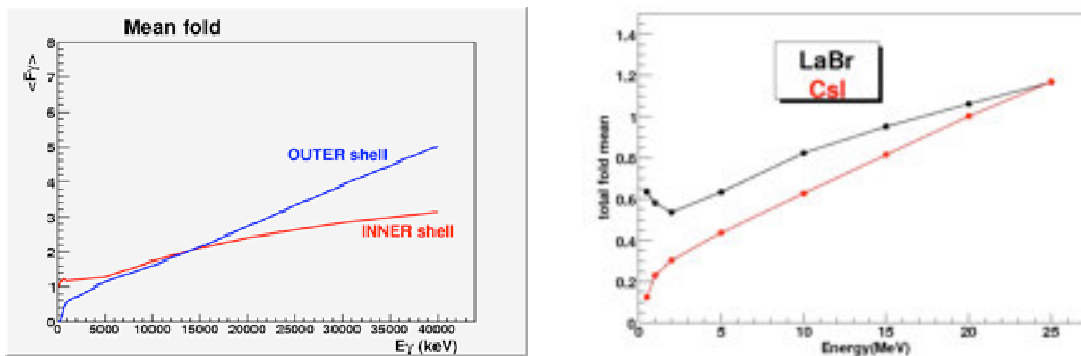


Fig. 9: Comparison of mean fold value for an ‘idea’ virtually segmented configuration (left) and a ‘wheel’ based arrangement (right)

The fold distribution, i.e. the number of crystals fired by a single  $\gamma$ -ray, is used to estimate how the energy is absorbed for a given geometry. Figure 9 compares the fold distribution as a function of the energy for the ‘ideal’ configuration with a virtual segmentation (225 elements) and the ‘wheel’ configuration (200 phoswiches elements). The latter configuration does not collect efficiently scattered photons which results in a mean fold smaller whatever the  $\gamma$ -ray energy. The fold distributions for the ‘cubic-like’ geometries (see fig. 10) have also been studied and the results are comparable with the ‘ideal’ case.

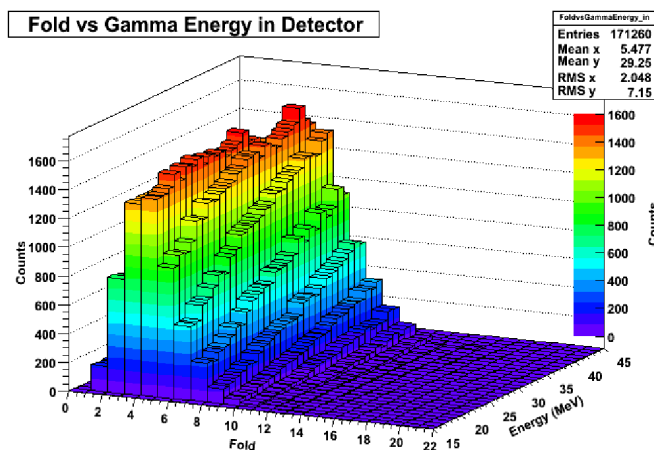
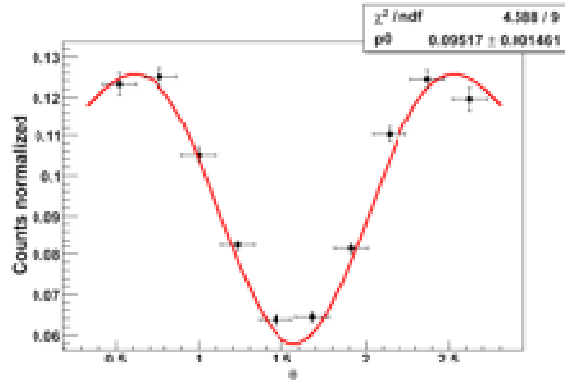


Fig. 10: Fold distribution as a function of the energy in a ‘cubic-like’ configuration

Coming back to the ‘wheel’ configuration, one of the major advantage is the quite uniform arrangement of the modules which permit precise determinations of angular distributions. It is illustrated in Fig. 11 where the response function to a non-isotropic emission is given, the horizontal error bars taking into account the opening angles of the detectors. The less isotropic and more compact ‘cubic-like’ configurations would probably give a less clean picture. So far, the different configurations have been studied using a source emitting a single  $\gamma$ -ray of various energies. Of course, in reality the sources are much complex and cascades of low energy  $\gamma$ -rays are emitted together with

one (or more) high energy  $\gamma$ -rays. Algorithms are needed to disentangle the different kind of emitted photons. An algorithm may be efficient for one geometry and not for another one since they are based on the way  $\gamma$ -ray are absorbed in the device. It is then difficult to guess which configuration would give the best response function for realistic events.



*Fig. 11: Response function of a 'wheel-like' configuration to an anisotropic emission*

What is quite well established is the way high energy  $\gamma$ -rays are absorbed : it requires an important depth of material. While the first interaction point is likely to occur in the first centimetres of LaBr<sub>3</sub>, the electromagnetic shower extends deeply and a second layer may be mandatory to get a large photo peak efficiency for GDR-like photons. It is important also, to get the true sum-spin value, to remove the contribution of the high energy  $\gamma$ -rays that interact, even partly, with the first layer.

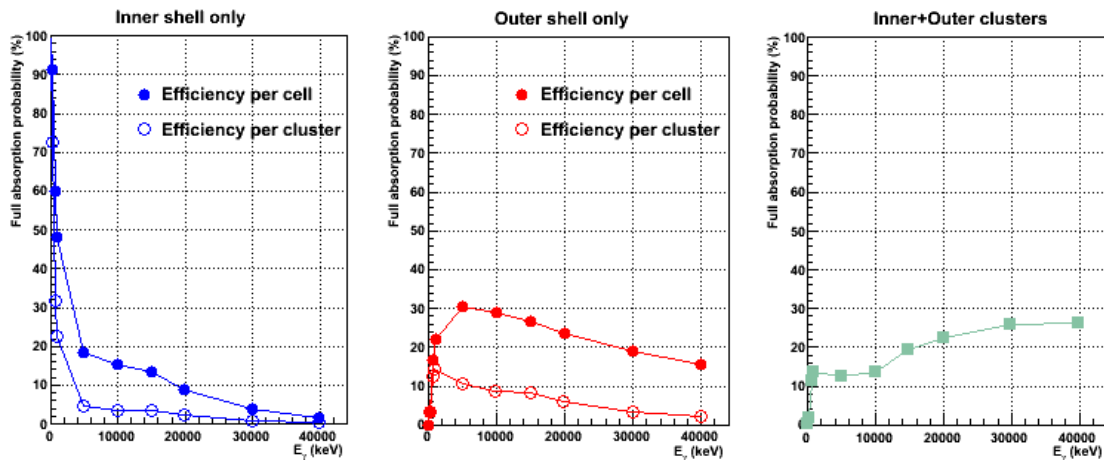


*Fig. 12: Efficiency of a basic clustering method in an 'ideal' configuration composed of two layers LaBr<sub>3</sub> and CsI.*

As it is illustrated in Fig 4, a considerable gain in the full absorption probability is expected by identifying and summing events that deposits their energy in the two layers. Some basic clustering methods have been tested for a single  $\gamma$ -ray in a 'ideal' configuration with a virtual segmentation (15x15). The results are displayed in Fig. 12. In this picture is given (the first two panels) what is expected without addback (efficiency per cell, open circles) compared to what is obtained by summing the closest neighbours of one segment (efficiency per cluster, full circles) in the inner and the outer shell. The last panel displayed the reconstruction efficiency we obtained by adding clusters in the two layers: it shows 28% in photo peak efficiency (at 40 MeV) could be gained from in-depth reconstructions.

Clustering methods have also been studied recently in the ‘cubic-like’ configuration (so far for one layer and with 2”x2”x4” crystals) in order to reconstruct a high energy  $\gamma$ -ray in a see of low energies. The results are given in Fig.13 and show a consequent improvement on the reconstruction of high energy  $\gamma$ -rays using the closest neighbours and this despite the cascade of low energy  $\gamma$ -rays.

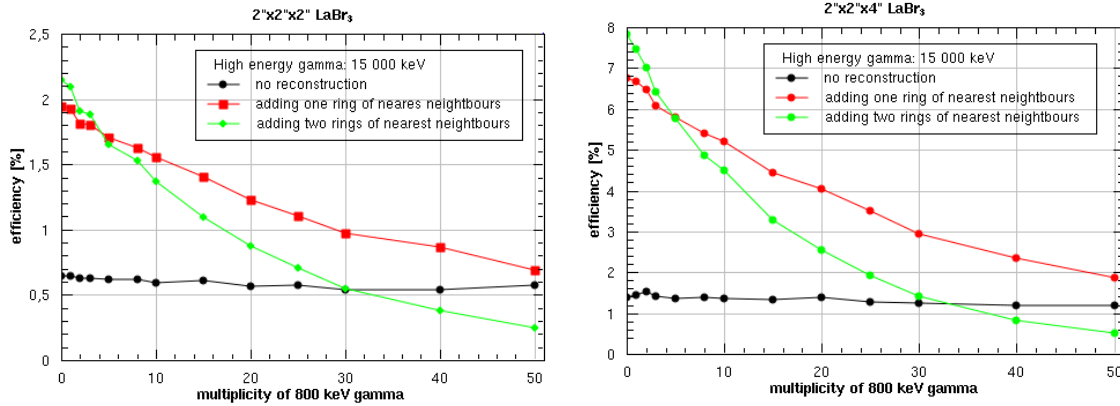


**Fig. 13:** Studies on clustering methods to reconstruct an high energy  $\gamma$ -ray in a “see” of low  $\gamma$ -ray photons in a ‘cubic-like’ arrangement

### 3. Conclusions

The response function has been extensively studied using as a reference an ‘ideal’ device composed of one and two concentric spheres. Building a compact array with the current available LaBr<sub>3</sub> shapes is quite difficult. Arrangement based on a spherical configuration (‘wheel’ like) suffers of a consequent loss of efficiency (compared to the ‘ideal’ case) at least for the inner part i.e. for the sum-spin spectrometric part. For high energy  $\gamma$ -rays, covering more space would improve the detection efficiency. A cubic like arrangement offers a better full absorption probability. However, the response function of such a device is more complicated to understand. Reconstruction algorithms, for  $\gamma$ -ray multiplicity greater than one, may suffer from this. Compact configurations based on different shapes of LaBr<sub>3</sub> crystals (if technically possible) is an interesting alternative.

The main parameters constraining the radial and angular segmentation of the full array have been studied in order to not deteriorate the good energy resolution provided by LaBr<sub>3</sub> crystals. These studies indicate an individual element should have an opening angle that does not exceed 20 degrees, a very good value being 6 degrees. It corresponds to a geometry with a few hundred of elements. Studies about clustering methods and reconstruction algorithms have just started and should provide the last results which would help to design the best configuration for the PARIS array.

This report synthesizes different simulation works. Detail studies could be found in the documents available at : <http://paris.ifj.edu.pl/documents/sim/>

## 2.3 Design and construction scheme

This part of the report summarizes the status of the mechanical scenarios working group for a spherical and cubic array. Different layouts have been discussed, they are presented for a 2 shells array, with a first shell composed of  $\text{LaBr}_3$  crystals.

**Spherical array** : The use for  $\text{BaF}_2\text{S}$  (Château de Cristal) is first described. The use of phoswich type modules is then explored in more details with 2 possible radii for the inner shell ( $R = 150 \text{ mm} / 70$  modules and  $R = 250 \text{ mm} / 200$  modules). A full 200 modules array is presented with PMTs and mechanical support for the total spherical array. GEANT4 simulations have been performed for the main proposed designs. Results are shown for the 70 and 200 phoswiches arrays. In particular, for the 70 modules array, we give results for absorption and gamma spectra. For the 200 modules array, results are given concerning gamma spectra, absorption in both shells, response to different multiplicities events (photopeak / total / add back), and to basic angular distributions.

**Cubic array and other shapes**: The proposal is to have an inner layer of  $\text{LaBr}_3$ , and an outer layer of CsI.

Detailed layouts are presented for cubic, decagonal and octadecagonal arrays.

### I Spherical shape scenarios:

The designs are based on  $\text{LaBr}_3$  cubic modules for the 1<sup>st</sup> layer of the **radial** array, coupled to a second shell of scintillators. Several possibilities are envisaged for this second shell: i. the use of existing  $\text{BaF}_2$  from the Château de Crystal, ii. the use of CsI crystals of different shapes in a phoswich configuration. Designs (sizes, radii, number of modules) have evolved according to discussions during the PARIS meetings and specific mechanics meetings.

All proposed spherical designs are optimized for a 5 mm minimum distance between the crystals for eventual canning and support and a 60 mm beam pipe of 1 mm thickness has been taken into account. All designs have been produced using **CATIA** mechanics software (Dassault Systems). Simulations have been performed using **GEANT4** ([www.cern.ch/geant4](http://www.cern.ch/geant4)).

### I.1. The 150 mm radius design:

#### I.1.1. First shell :

The first design we have studied is a 150 mm radius design for a first shell. Using 2''x2''x2''  $\text{LaBr}_3$  modules, this results in a 70 modules spherical array and is shown in Fig. 1. The corresponding solid angle for these 70 modules is 8 sr.

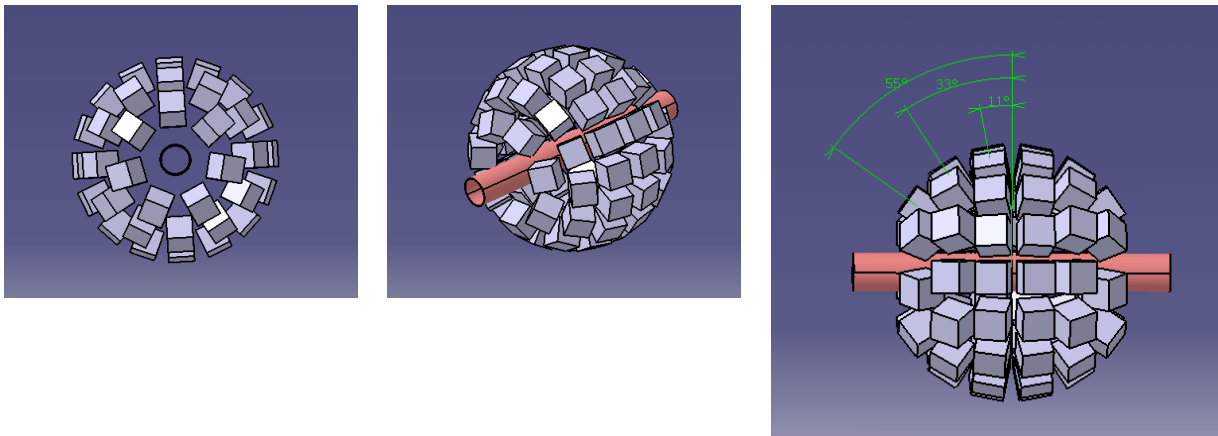


*Fig. 1. : Inner shell of the 150 mm configuration with 70  $\text{LaBr}_3$  modules.*

A summary of the characteristics of this first layer is presented in Table 1.

	Nb of detectors	Min. distance between det. (mm)	Distance to next ring (mm)
Ring 1 (55°)	7	10.9	5.9
Ring 2 (33°)	12	8.9	6.9
Ring 3 (11°)	16	5.8	7.4

**Table 1.** : Details about the 150 mm configuration with 70  $\text{LaBr}_3$  2''x2''x2'' modules.

GEANT4 calculations for this configuration are presented below together with calculations for the second shell (Fig. 7 and 8).

### I. 1.2. Second shell :

#### I. 1.2.1. $\text{BaF}_2$ :

The first possibility we discussed was the use of existing  $\text{BaF}_2$  modules from the Château de Cristal which design was made by the Strasbourg mechanical design workshop, so that original designs have been used (see Fig. 2). A 10 mm space has been left between the shells to allow the use of PMTs (APDs) for the  $\text{LaBr}_3$ .

An optimized configuration would take advantage of a maximum number of modules and would contain 102  $\text{BaF}_2$  modules. It is presented in Fig. 3. The solid angle covered by 102  $\text{BaF}_2$  is 8 sr

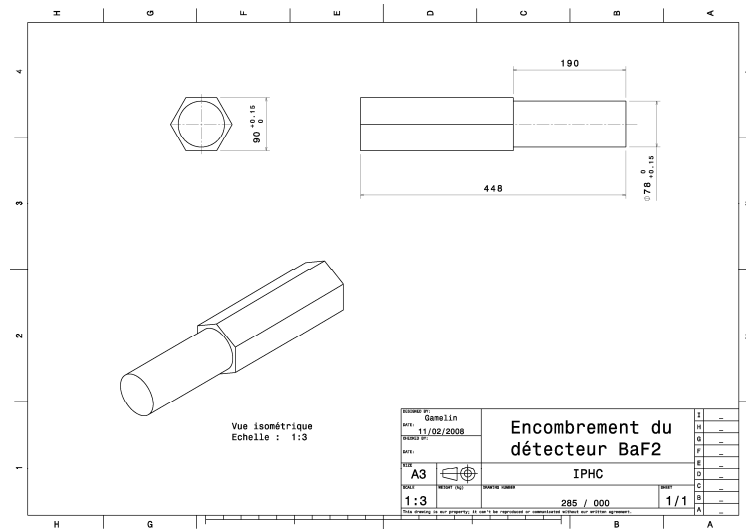


**Fig. 2.** :  $\text{BaF}_2$  detector design for the Château de Cristal detectors (IPHC Strasbourg workshop).

At the moment, 68 modules from the Château de Cristal are available and thus Fig. 4 shows a more realistic design with 68  $\text{BaF}_2$  detectors. The corresponding solid angle is 7.6 sr.

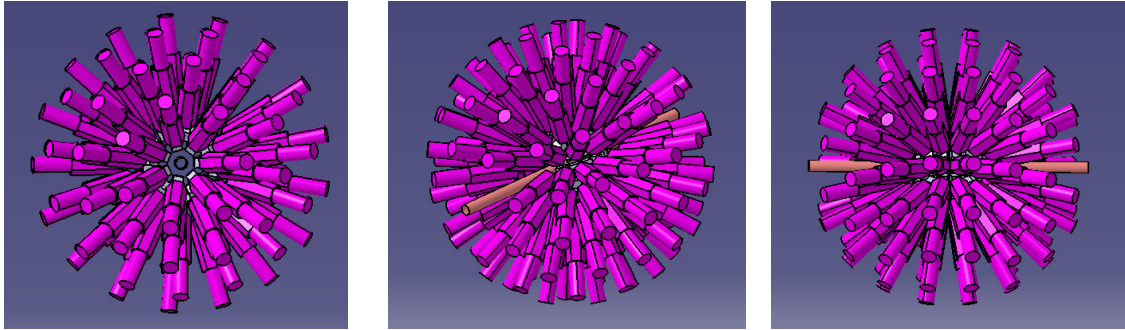


**Fig. 3.** : CATIA 2 shells configuration with 70  $\text{LaBr}_3$  modules and 102  $\text{BaF}_2$  scintillators of Château de Cristal type.

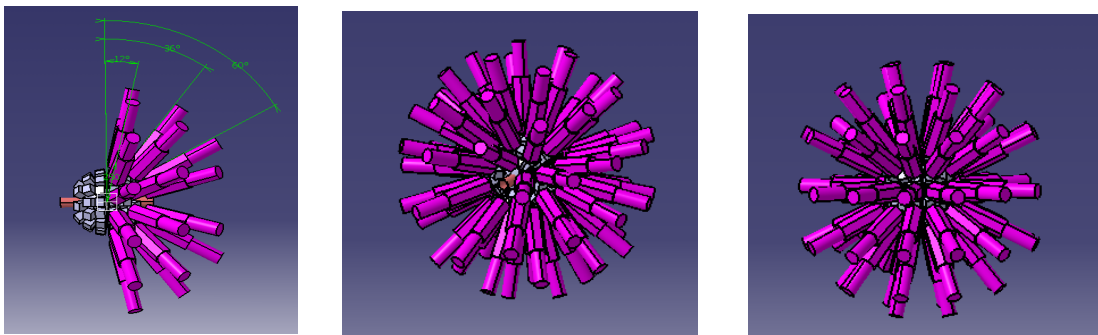


**Fig. 4.** : CATIA 2 shells design with 70  $\text{LaBr}_3$  modules and 68  $\text{BaF}_2$  detectors of Château de Cristal type.

#### I. 1.2.2. CsI :

This part discusses a phoswich type mechanical design with a first  $\text{LaBr}_3$  shell of  $2'' \times 2'' \times 2''$  crystals. The second shell is made of CsI crystals of  $6''$  length. The IPHC workshop has produced several designs based on different possible shapes for the CsI modules.

- 70  $\text{LaBr}_3$  ( $2'' \times 2'' \times 2''$ ) and 70 CsI ( $2'' \times 2'' \times 6''$ )

This design is made of the 150 mm radius first shell described above and a second CsI shell in a phoswich type configuration. The CATIA design is shown in Fig. 5. Details on the geometry are the same as in Table 1, since this configuration uses the same  $\text{LaBr}_3$  first shell.

**GEANT4** simulations have been performed for such a configuration (Fig. 6). These simulations are based on the mechanical step files for the definition of the geometry used in the code. The step files are converted into **GDML** (Geometry Description Markup Language / [www.cern.ch/gdml](http://www.cern.ch/gdml)) files using the **Fastrad** software. GEANT4 GDML package needs to be installed for these types of calculations. Materials are defined by the user. Basic results of these simulations are presented below such as absorption and photopeak absorption for each shell and examples of simulated spectra. These results are in agreement with the article of Niccolini *et al.*<sup>2</sup>. More advanced simulations have been performed for the 200 detectors configuration and are presented in the corresponding part of this report. The photopeak absorption (sum of all detectors of the same

<sup>2</sup> Niccolini *et al.*, Nucl. Inst. Methods A **582** (2007) 554.

material) is presented in Fig. 7. This Figure compares to the dashed curves in Fig. 16 for 200 modules. Fig. 8 shows examples of  $\gamma$  spectra in both shells.

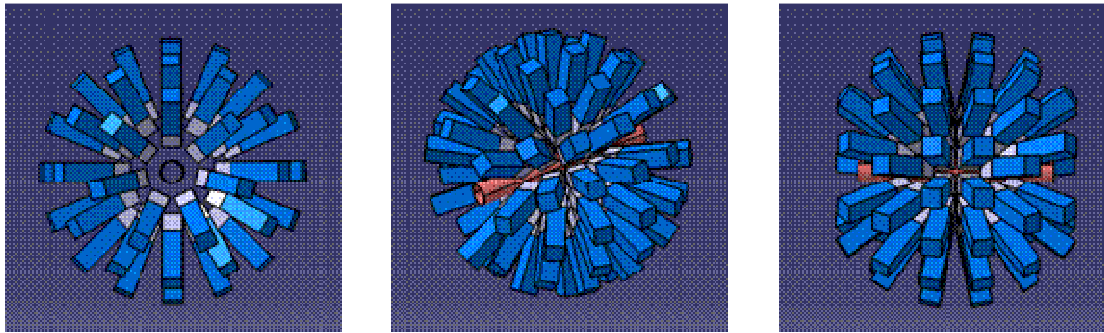


*Fig. 5. : Phoswich type design with 70  $\text{LaBr}_3$  +  $\text{CsI}$  modules.*

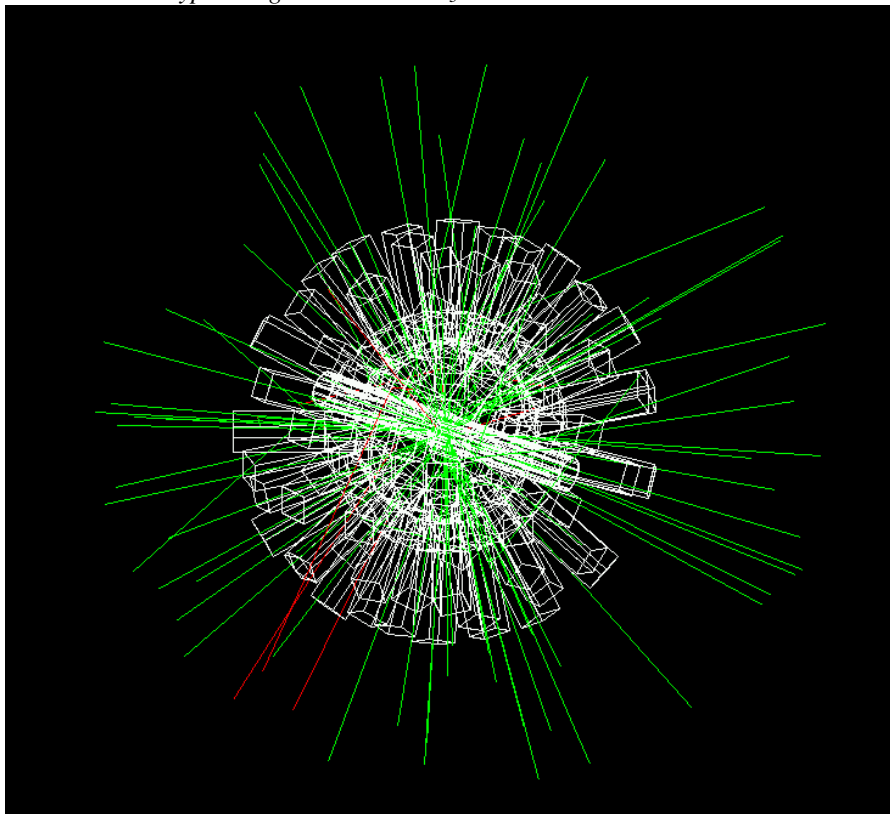


*Fig. 6. : GEANT4 simulation for the 70 phoswiches (150 mm inner radius) + 60 mm beam pipe configuration : geometry and 100 tracks (green for gammas and red for electrons).*

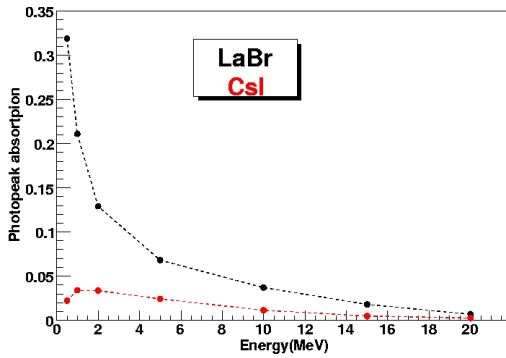


**Fig. 7. :** GEANT4 simulation for the 70 phoswiches. Photopeak absorption in the  $\text{LaBr}_3$  and CsI shells, with sum of all detectors (add back).

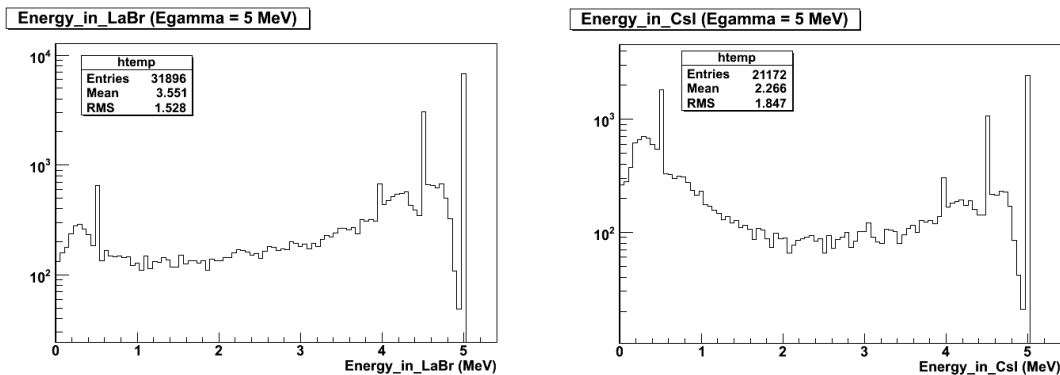


**Fig. 8. :** GEANT4 simulation for 70 phoswiches (150 mm radius). Examples of simulated spectra for 100000 events. More advanced simulations will be presented for the 200 detectors configuration.

The shape of the second layer may be changed to tapered to gain angular coverage. This is presented in the next paragraph.

- 70  $\text{LaBr}_3$  (2''x2''x2'') and 70 CsI (tapered)

Two designs have been proposed. These configurations are still based on 70 telescopes and a minimum distance between detectors is kept to 5 mm.

The first design (a.) is based on a CsI cristal with a 2''x2'' side 'glued' to the  $\text{LaBr}_3$  cristal and 6'' length. Details are given in Fig. 9 and the full array is shown in Fig.10. The second design, design (b.), is based on larger dimensions (60x60 mm<sup>2</sup>) for the side 'glued' to the  $\text{LaBr}_3$  and a 6'' length. It is presented in Fig. 11 and 12.

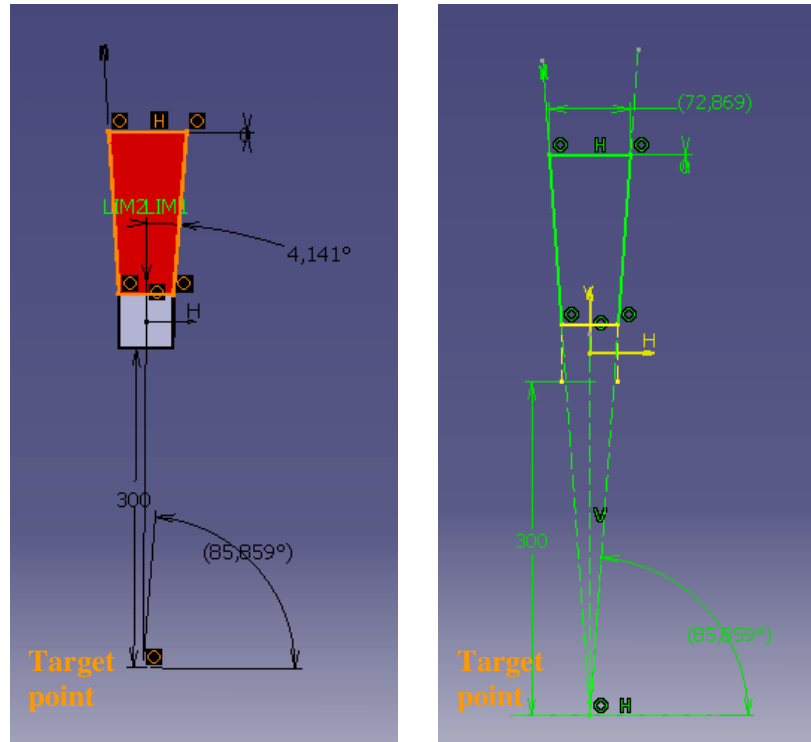


*Fig. 9. : Example of a  $LaBr_3$  + tapered CsI module for the design a.*

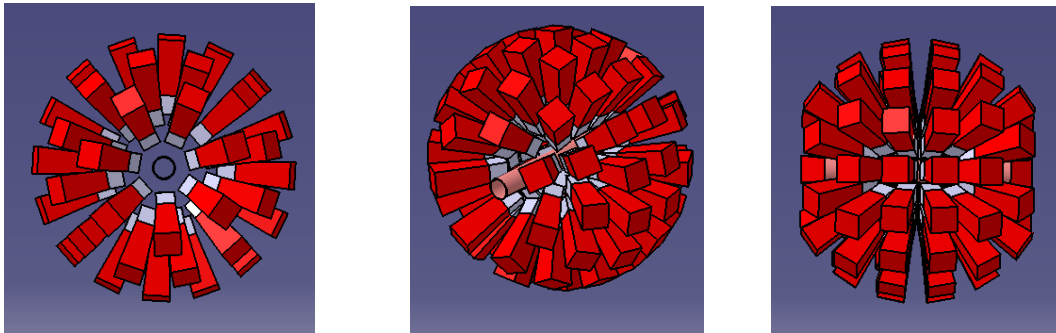


*Fig. 10. : Full array of 70 modules as presented in Fig. 7, design a.*

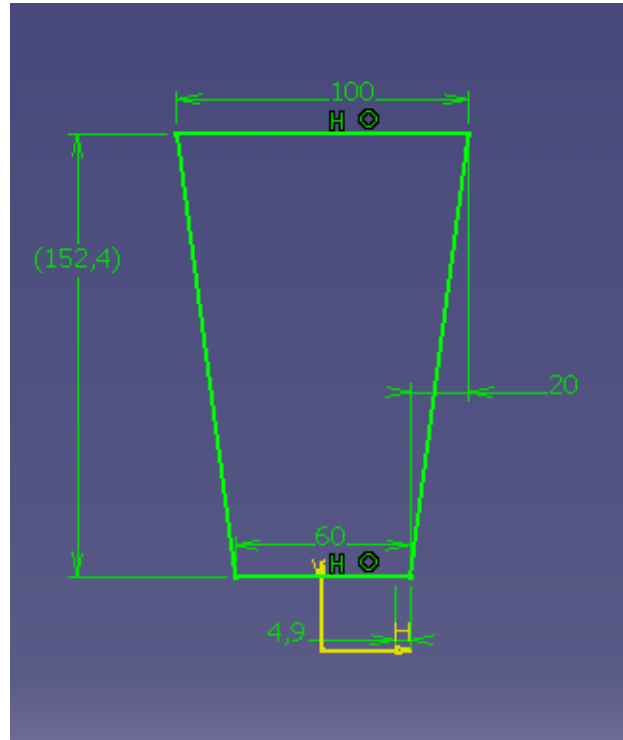


**Fig. 11.** : Size of the CsI tapered modules tapered for the design b.

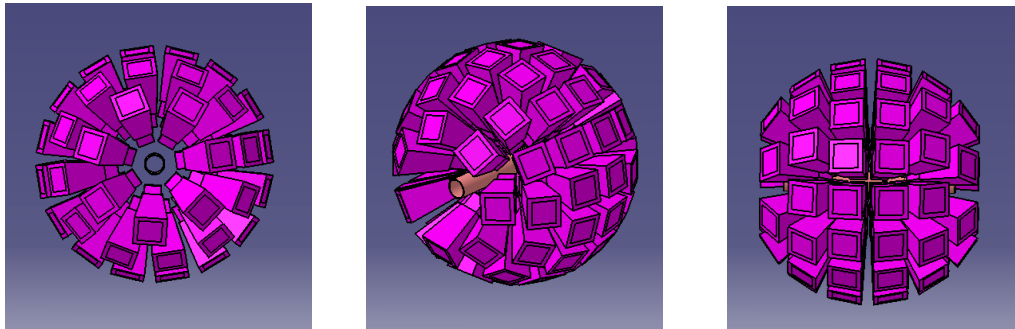


**Fig. 12.** : CATIA design (b.) for the full array of 70 modules (LaBr<sub>3</sub> 2''x2''x2'' + CsI as presented in Fig. 7).

Numerical simulations for designs a. and b. have not been performed yet. It has been discussed in the last PARIS meeting (York, May 2008) that priority should be given to a 200 modules design. This design is presented in the next part along with up to date simulations of absorption, multiplicity reconstruction, reconstruction of specific angular distributions. Resolution has been implemented in the spectra as measured up to 17.6 MeV by M. Ciemala *et al.* in the PARIS collaboration.

### **1.2. The 250 mm radius design (200 phoswiches):**

This 250 mm radius corresponds to 200 LaBr<sub>3</sub> 2''x2''x2'' crystals mapping a sphere (with a 5 mm minimum distance between the modules) and 200 CsI crystals 2''x2''x6''. The solid angle for the LaBr<sub>3</sub>'s is 8.26 sr. The design is presented in Fig. 13.

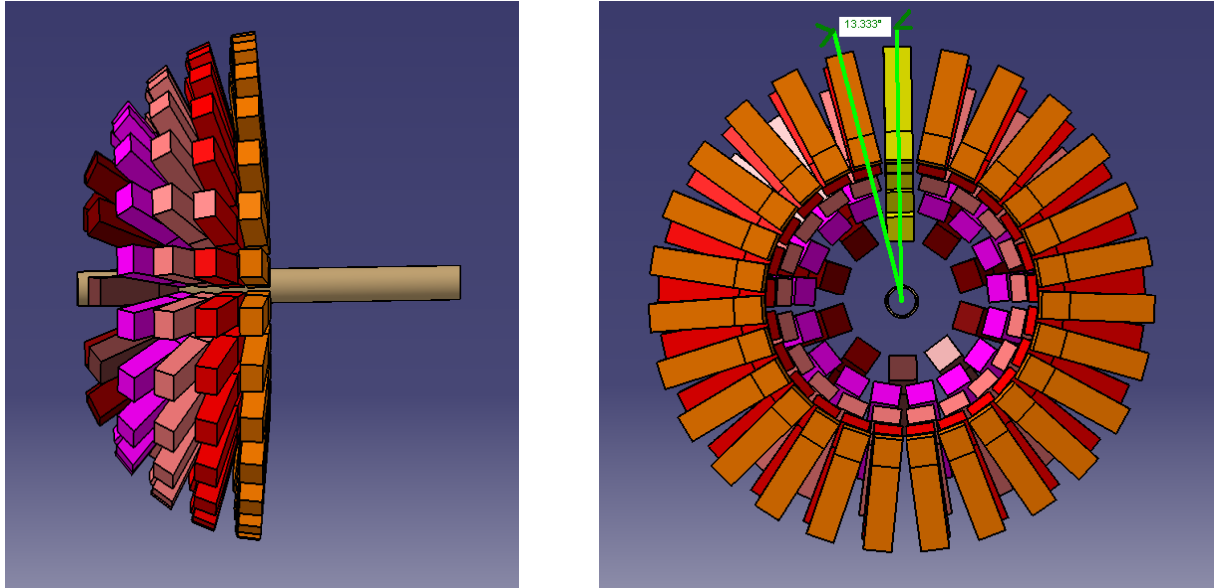


**Fig. 13.** : CATIA design for the 200 detectors geometry. Two half spheres of 100 phoswiches are presented here.

Fig. 14 shows details about the angles between the different rings of such an array.

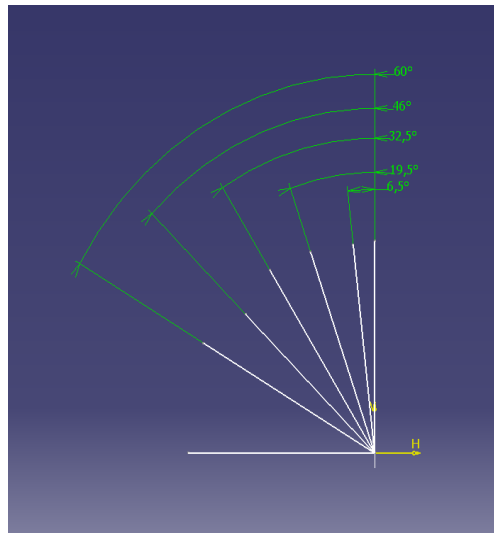


**Fig. 14.** : Angles corresponding to the rings with respect to the axis perpendicular to the beam pipe.

Details about the design of the array with 200 modules are given in Table 2.

	Number of detectors	Angle between det. of the ring (°)
<i>Ring 1</i>	27	13.3
<b>Ring 2</b>	25	14.4
<b>Ring 3</b>	21	17.1
<b>Ring 4</b>	17	21.2
<b>Ring 5</b>	10	36

**Table 2:** Configuration with 200 phoswiches mapping a sphere of 250 mm radius. This concerns one half of the array, the other half being symmetrical.

GEANT4 simulations have been performed for this design. The geometry has been defined with the CATIA step files. Results are given below for this 200 phoswiches configuration.

For multiplicity 1 of the events, figure 11 shows the photopeak absorption, when the photopeak energy is deposited in one crystal only.

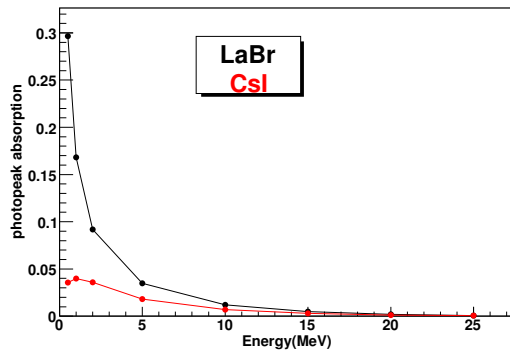


**Fig. 15. :** GEANT4 simulation. Photopeak absorption for the 200 phoswiches in  $\text{LaBr}_3$  and in CsI. The photopeak is detected in one cristal only (no add back).

Fig. 16 shows the photopeak absorption when the photopeak energy is selected in a sum of all  $\text{LaBr}_3$  or CsI spectra, i.e. a perfect add back inside the  $\text{LaBr}_3$  or CsI material..

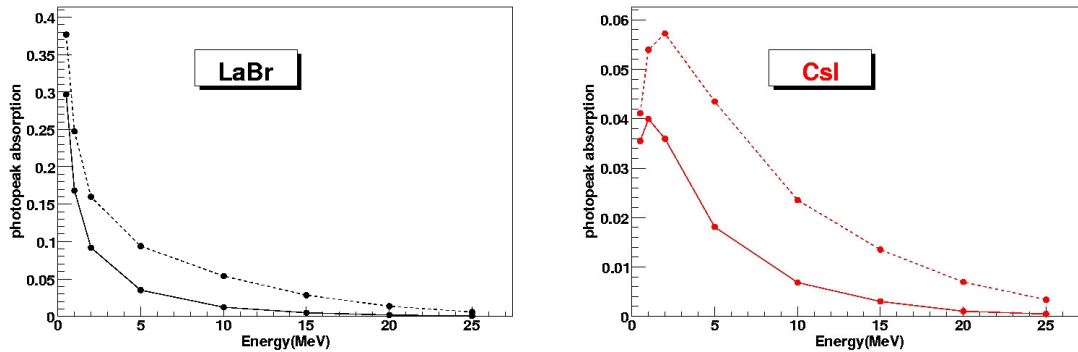


**Fig. 16. :** GEANT4 simulation. Dashed curve : photopeak absorption (perfect add back) for the 200 phoswiches configuration. The plain curve corresponds to no add back.

Fig. 17 shows the mean fold (number of detectors fired) as a function of the energy for events of multiplicity 1. Pair production, photopeak effect and Compton effet contribute to this mean fold: it can thus be larger than the multiplicity.

In simulations of 100000 events of multiplicity 1, the maximum fold we observe is 10 (res. 8) in the  $\text{LaBr}_3$  (resp. CsI) for  $E_\gamma = 5$  MeV and it is 13 (resp. 9) in the  $\text{LaBr}_3$  (resp. CsI) for  $E_\gamma = 25$  MeV.

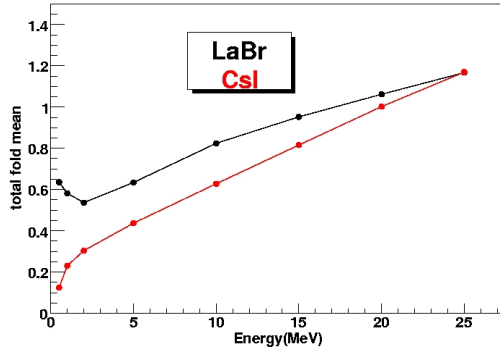


**Fig. 17.** : GEANT4 simulation. Mean fold as a function of the energy for events of multiplicity 1, for the 200 phoswiches configuration.

Simulations for multiplicity 1 to 30 have also been performed. They are presented below.

Fig. 18 shows the mean photopeak fold as a function of the multiplicity of the events, for multiplicities ranging from 1 to 30 and for different energies (0,5-1-2 and 5 MeV).

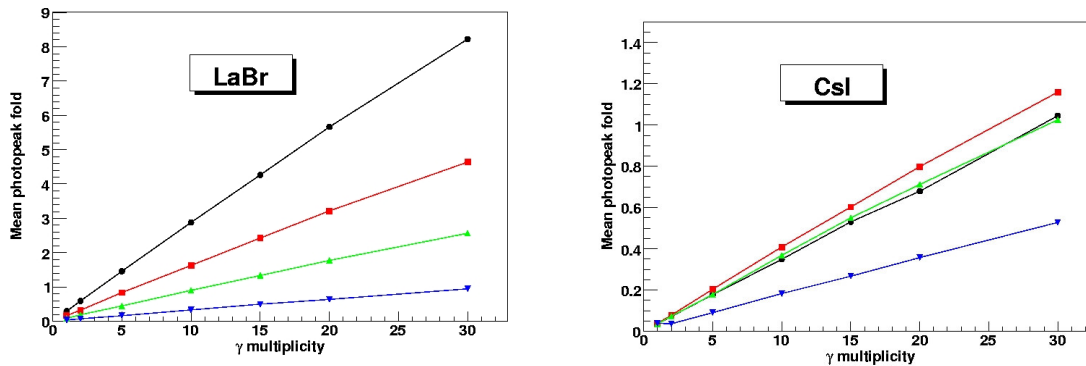


**Fig. 18.** : GEANT4 simulation. Mean fold (photopeak) as a function of the  $\gamma$  multiplicity in the LaBr and CsI for several energies : 0.5 MeV (black), 1 MeV (red), 2 MeV (green) and 5 MeV (blue).

In simulations of 100000 events, for cascades of 20  $\gamma$ -rays, the fold reaches 12 (resp. 4) in LaBr<sub>3</sub> (resp. CsI) for  $E_\gamma = 0.5$  MeV; it can reach 5 (resp. 4) for  $E_\gamma = 5$  MeV

The mean photopic fold divided by the multiplicity is given in Fig. 19 for the LaBr<sub>3</sub>. It is slowly decreasing over the range mult = 1 to mult = 30. This almost flat behaviour reflects the LaBr<sub>3</sub> efficiency.

Fig. 20 shows the mean fold for the full  $\gamma$  spectra (photopeak energy selection) as a function of the multiplicity for  $E_\gamma = 0.5$ -1-2 and 5 MeV. Simulations have been performed for the maximum fold for several multiplicities. In simulations of 100000 events, for cascades of 20  $\gamma$ -rays, the maximum fold in LaBr<sub>3</sub> (resp. CsI) is 30 (resp. 22) for  $E_\gamma = 0.5$  MeV, it is 25 (resp. 20) for  $E_\gamma = 5$  MeV.

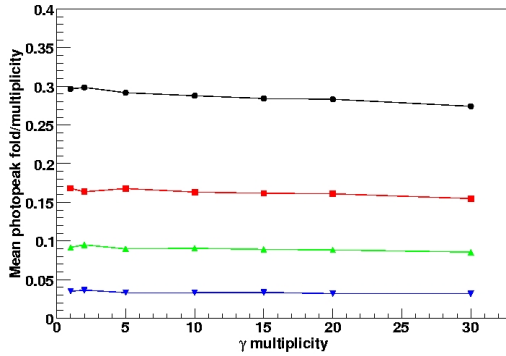


Fig. 19. : GEANT4 simulation. Mean photopeak fold divided by the multiplicity for the LaBr<sub>3</sub> detectors as a function of the multiplicity of the events for several energies: 0.5 MeV (black), 1 MeV (red), 2 MeV (green) and 5 MeV (blue).

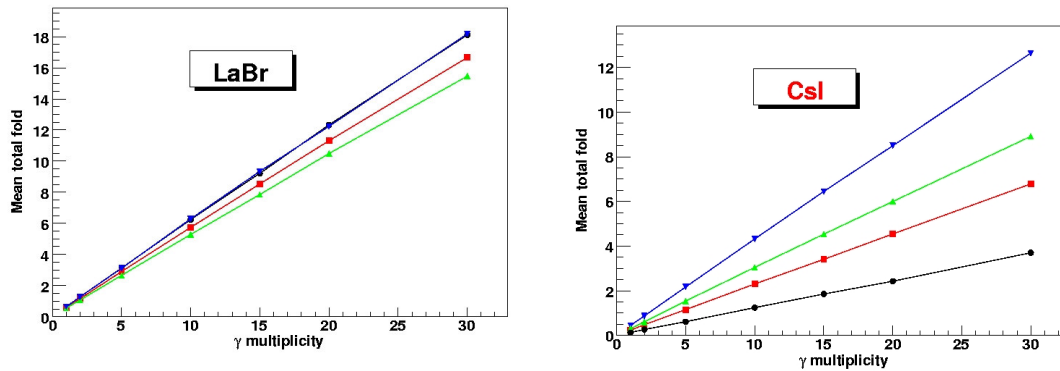


Fig. 20. : GEANT4 simulation. Mean fold as a function of the  $\gamma$  multiplicity for  $E_\gamma = 0.5$  MeV (black), 1 MeV (red), 2 MeV (green) and 5 MeV (blue).

Fig 21. shows the example of a simulated spectrum (sum of the 200 LaBr<sub>3</sub>s) for 5 MeV events convoluted with experimental resolution.

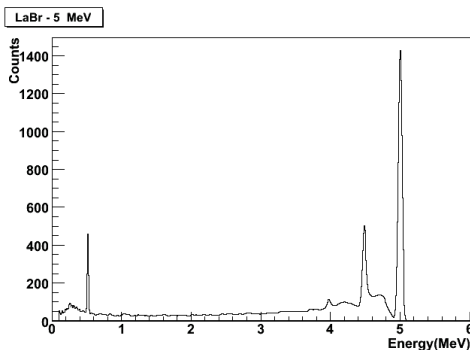
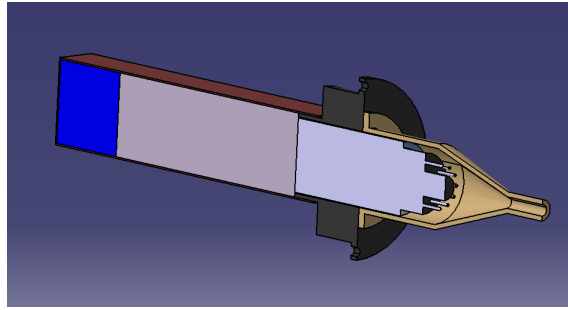


Fig. 21. : GEANT4 simulation of 100000 events. Gamma spectrum in the 200 LaBr<sub>3</sub>s for 5 MeV events with convolution with experimental resolution.

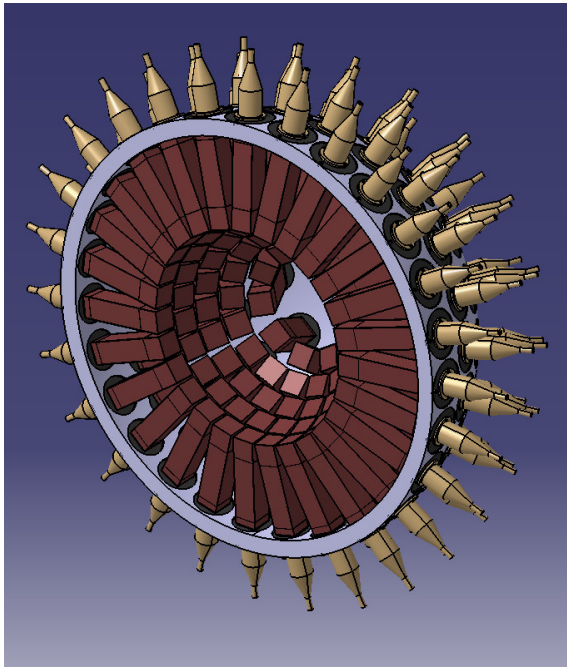
The next part of this report shows the design for the 200 detectors configuration with full support of the spherical array, canning of the detectors with 1 mm carbon foils and R580 Hamamatsu PMTubes. Please note that a **double readout** of the signals could be envisaged with **APDs** on 1 side of the LaBr<sub>3</sub> crystal. Test of LaBr<sub>3</sub> coupled to APDs are in progress at IPHC, Strasbourg.

Fig. 22 presents one of the 200 detectors.



**Fig. 22.** : CATIA layout of a LaBr<sub>3</sub> (2''x2''x2'') + CsI (2''x2''x6'') coupled to a R580 PMT (Hamamatsu).

Fig. 23 to 25 show the full array radial layout with total spherical support. The distance from target to LaBr<sub>3</sub> is still 250 mm.



**Fig. 23.** : CATIA layout of a half sphere array with 100 phoswiches.

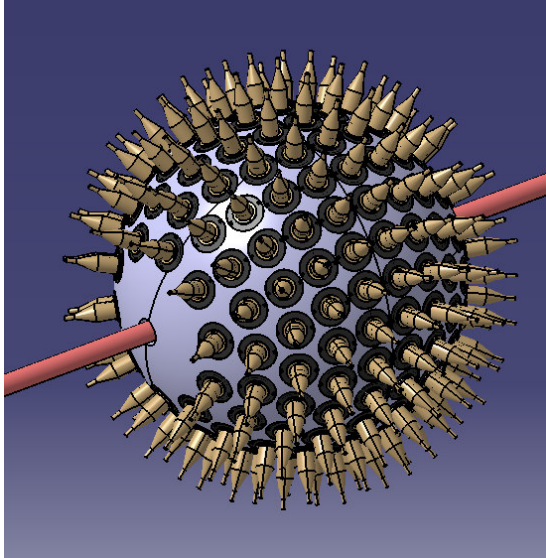


*Fig. 24. : CATIA layout of the full spherical array with 200 detectors.*

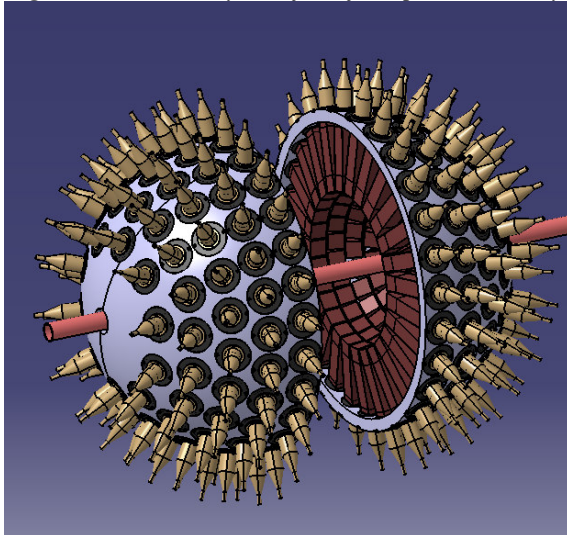


*Fig. 25. : CATIA layout of the full spherical array with 200 detectors.*

The next paragraph concerns the reconstruction of angular distributions for such a spherical array (10 rings). Simulated angular distributions are presented in Fig. 26 to 28. Fig. 26 shows the response to a uniform distribution of the  $\gamma$ -rays.

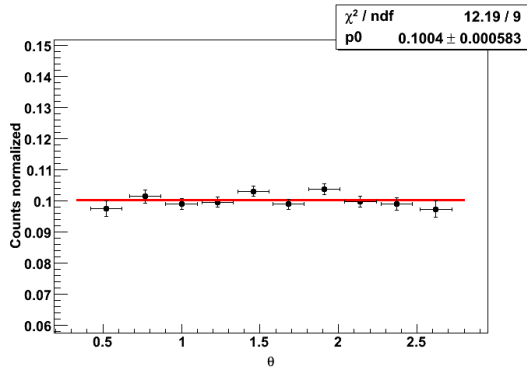


**Fig. 26. :** GEANT4 simulation of 100000 events. Response of the 200 detectors array to a uniform distribution for 0.5 MeV  $\gamma$ -rays (angle in radians). Error bars take into account the opening angle of detectors and number of simulated events.

Fig. 27 shows the response to  $4^+ \rightarrow 2^+$  transitions and Fig. 28 the response to  $2^+ \rightarrow 0^+$  transitions.

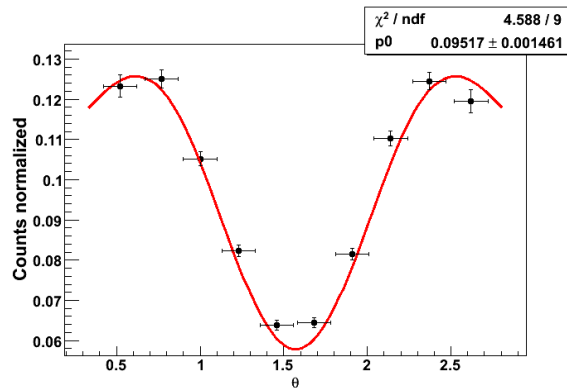


**Fig. 27. :** GEANT4 simulation of 100000 events. Response of the 200 detectors array to  $4^+ \rightarrow 2^+$  transitions for 0.5 MeV  $\gamma$ -rays (the red curve is represents the theoretical distribution, the angle is in radians). Error bars take into account the opening angle of detectors and number of simulated events.

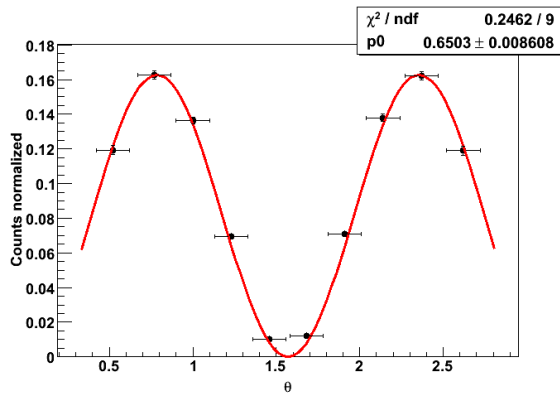


**Fig. 28.** : GEANT4 simulation of 100000 events. Response of the 200 detectors array to  $2^+ \rightarrow 0^+$  transitions for 0.5 MeV  $\gamma$ -rays (the red curve is represents the theoretical distribution, the angle is in radians). Error bars take into account the opening angle of detectors and number of simulated events.

Simulations show a very good reconstruction of these basic angular distributions. No add back has been made: the shape of the distribution does not depend on the energy of the  $\gamma$ -rays. Errors on the distributions increase, in principle with the add back procedure. This is to be investigated. The reconstruction of different distributions could of course be investigated for specific physics cases.

## II . Cubic shape arrays :

### II 1. Introduction

The brief is to study how best to position Lanthanum Bromide and Caesium Iodide crystals to realise a cost effective detector array. The proposal is to have an inner layer of  $\text{LaBr}_3$ , and an outer layer of  $\text{CsI}$ . This part focuses on the design of a cubic shaped array.

### II 2. Detector Design

#### II 2.1 Lanthanum Bromide limitations

Lanthanum Bromide is a relatively newly discovered scintillator and it is difficult to realise crystals larger than 2" in size and the most cost effective way to purchase these crystals is in cubic form. In order to operate as a detector the crystals have to be held in a light-tight container with the signals read out electronically.

There are two ways to read signals from lanthanum bromide, via Photo-multiplier tubes (PMTs) or Large Area Avalanche Photodiodes. Large Area Avalanche Photodiodes, initially seemed promising as they are much smaller in size than PMTs, however they require alcohol cooling

#### II 2.2 Caesium Iodide limitations

Caesium Iodide is a relatively mature technology, and relatively large crystals can be grown if required. It is also relatively easy to shape these crystals after they have been grown as required. Similarly to  $\text{LaBr}_3$  the crystals have to be held in a light tight container with the signals read out electronically. As there is more space behind the Caesium Iodide, PMTs should be used to read out the signals.

The most cost effective way to purchase these crystals is in cubic form, and hence it seems reasonable to assess the viability of a cubic array.

### II 2.3 Detector layout

Four options were considered Separated crystals, combined crystals with single readout, combined crystals with dual readout and combined shaped crystals.

#### II 2.3.1 Separated crystals

This concept was to have separated crystals with the  $\text{LaBr}_3$  crystals read out separately to the  $\text{BaF}_2$  crystals. This has been rejected in favour of the combined options which are more compact, and have no material between the crystals.

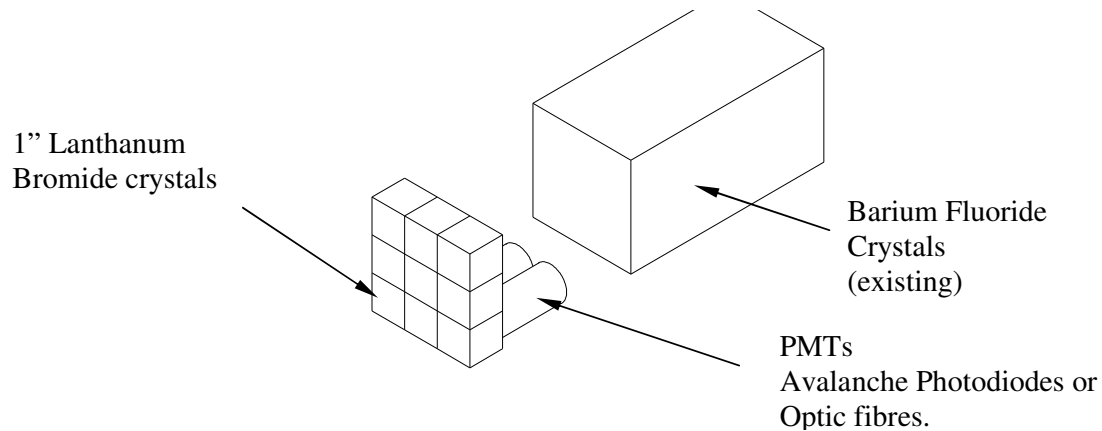


**Fig.29.** Separated crystals

#### II 2.3.2 Combined crystals with single readout.

It is possible to bond a  $\text{LaBr}_3$  crystal directly to a doped  $\text{CsI}$  crystal, and because the frequency of light emitted by the different materials are discrete, one can establish which crystal interacted with the particle by looking at the wavelength of the light. Hence a single Photo-Multiplier Tube can be used to read and differentiate the light from both crystals giving a design as shown below. This style of detector has been called a telescope (phoswich).

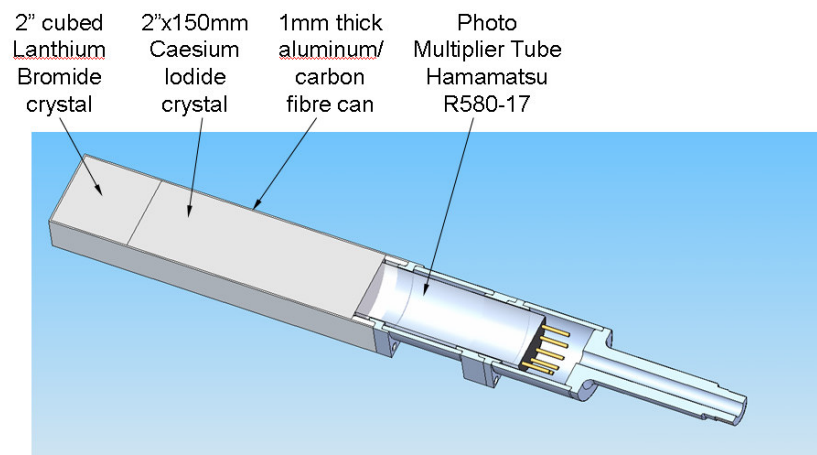


**Fig.30.** Combined crystal with single readout.

#### II.2.3.3 Combined crystals with dual readout

This concept uses the same  $\text{LaBr}_3$  crystal bonded to a  $\text{CsI}$  crystal as discussed in section II. 2.3.2, however an additional readout device (probably a photo avalanche diode) is attached to the front face of the Lanthium Bromide crystal. This gives timing benefits over the single readout option.

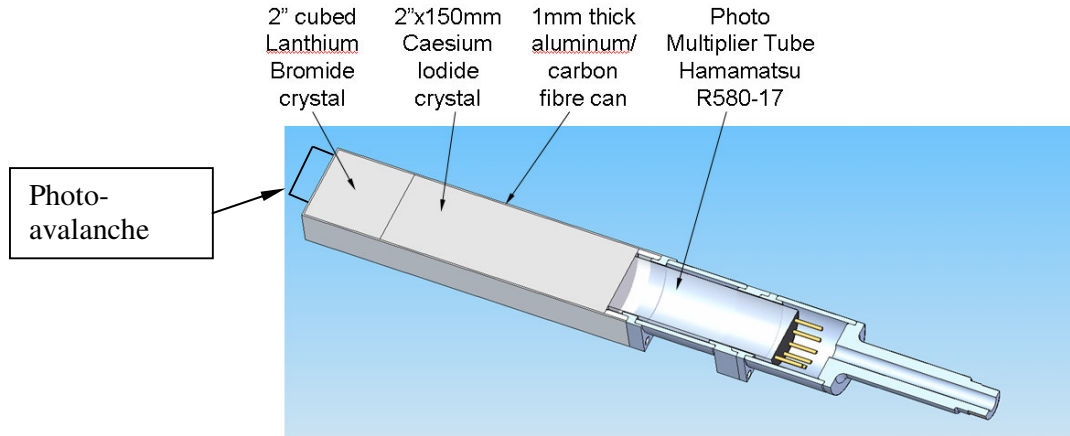


*Fig.31. Combined crystal with dual readout.*

#### II. 2.3.4 Combined shaped crystals.

The proposal here is to make crystals of similar shape to the AGATA crystals, to give similar angular coverage to that achieved by the AGATA detectors, and to serve as a benchmark.

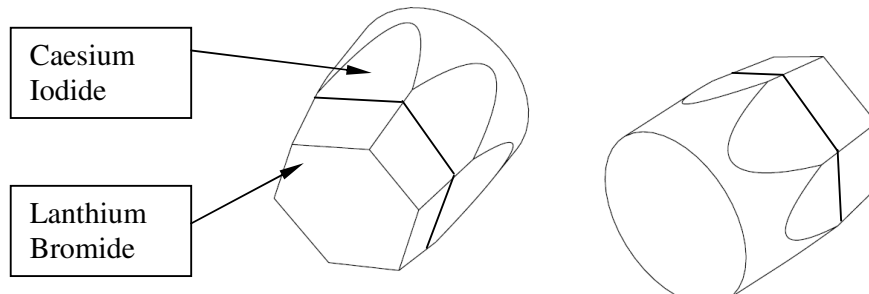


*Fig.32. Combined shaped crystal*

This crystal type is more suited to a radial array (see section II 1.2.2., tapered CsI).

### II. 3. Detector Array Design

This report focuses on a cubic array design.

It was decided to focus on the combined crystal, or telescope type detector, to study this array.

Initially work focussed on how many 2" cubic detectors could be fitted around different inner radius sizes.

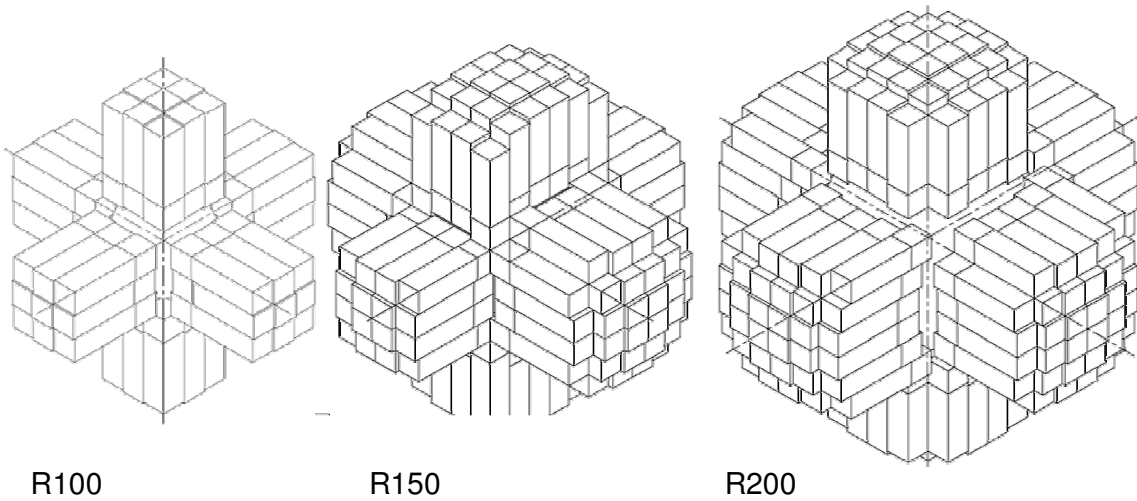


**Fig.33** Initial cubic detector arrays, R100 shows 54 crystals around a 100mm radius internal sphere, R150 shows 144 crystals around a 150mm radius internal sphere, R200 shows 200 crystals around a 200mm radius internal sphere

At the International meeting in York it was decided to assume that we could afford to purchase 200 detectors, and to study the different array possibilities that could be constructed using a cubic style array with 200 detectors to find the most efficient array style. And so the following array types were generated: Cubic – 6 sides, Decagonal – 10 sides, Octadecagonal – 18 sides.

Co-ordinates of the crystals were generated from the cad data so that the arrays could be rebuild an simulated in GEANT4.

### II. 3.1 Cubic Layout

This array has 6 faces. It has an inner sphere of radius 235mm with a beam pipe of 60mm diameter. It uses 208 telescopes.

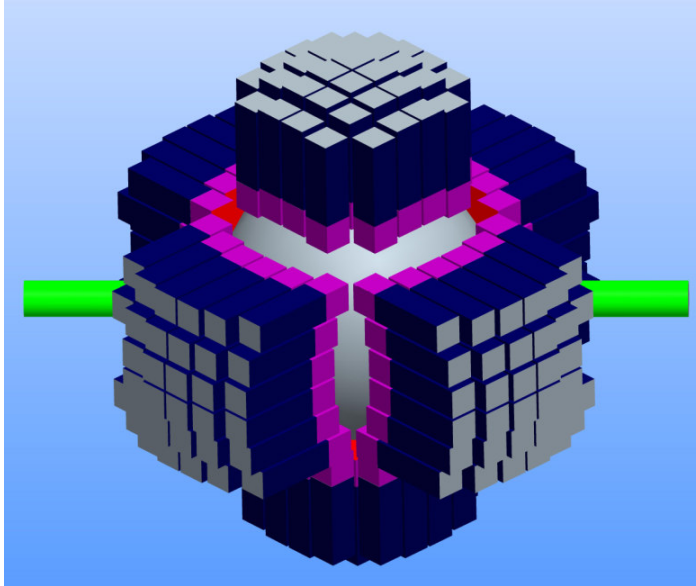


*Fig.34. R235 Cubic array*

### *II. 3.2 Decagonal Layout*

This array has 10 faces. It has an inner sphere of radius 235mm with a beam pipe of 60mm diameter. It uses 200 telescopes.

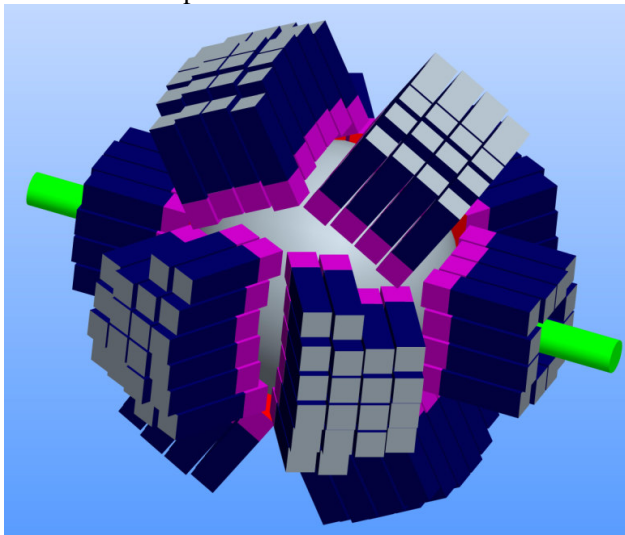


*Fig.35. R235 Decagonal array.*

### *II. 3.3 Octadecagonal Layout*

This array has 18 faces. It has an inner sphere of radius 235mm with a beampipe of 60mm diameter. It uses 196 detectors.

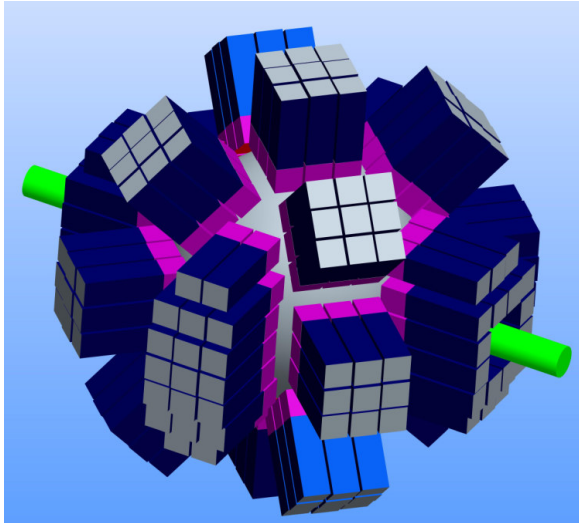


*Fig.36. R235 Octadegonal layout*

#### II. 4. Detector Structural Design

The design on an individual detector was examined to see if it was possible to design a mounting structure for a cubic type crystal.

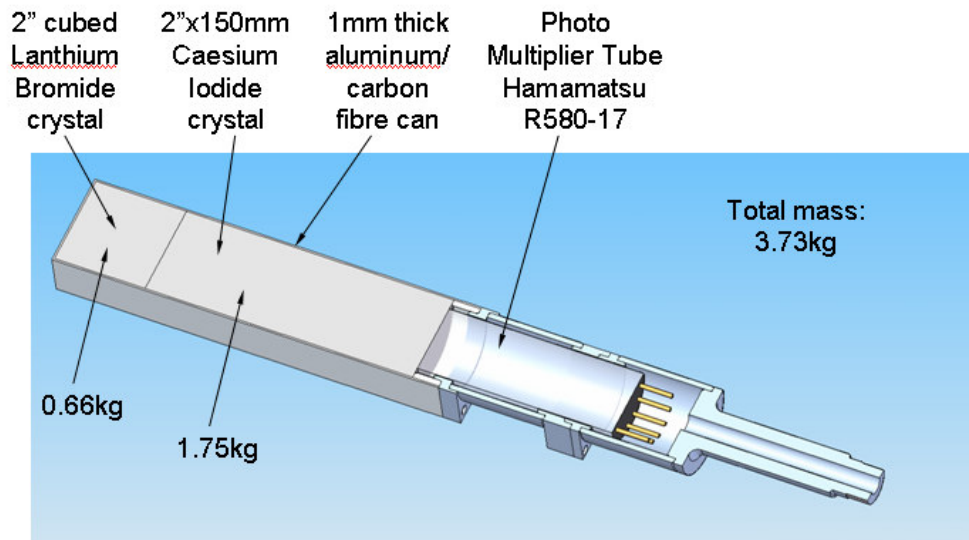


*Fig.37. Cubic detector layout.*

The design proposed is shown in figure 37. where the crystals are supported from the rear. This allows a 'wall' or detectors to be built up, and several of these 'walls' could be combined to form a detector array.

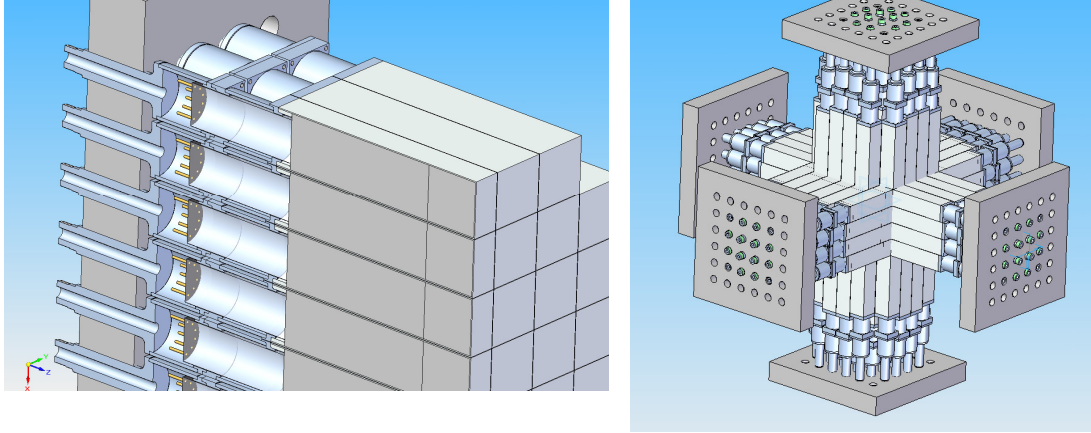


**Fig.38.** Array layout.

### III. Future plans

Concerning the radial array, we will study other possibilities for the support of the total array and also envisage the use of 4''x4''x4'' LaBr<sub>3</sub>. The next step for the simulations we have presented here, is to define an add back procedure and simulate specific physics cases involving cascades of  $\gamma$ -rays with different energies and angular distributions. The future plans will be discussed in our next PARIS WG meeting during the Spiral 2 week in Caen in January 2009 and in the PARIS Collaboration meeting in Krakow.

#### 2.4 Calibration procedures

##### Detectors testing:

Three main options have been chosen to define the best issue of the final detector type which will be used for the PARIS project :

- a two-shell detector composed of a first stage (LaBr<sub>3</sub>:Ce crystal) coupled to a photodetector (in that case, the thinner will be the best such as LAAPDs, SiPMs, ...) and of second stage with such a large CsI(Na) or BaF<sub>2</sub> crystal coupled with a PM tube.
- a telescope detector composed of LaBr<sub>3</sub>:Ce crystal followed by a large CsI(Na) coupled to a PM tube.
- a large LaBr<sub>3</sub>:Ce crystal coupled with a PM tube, or even possibly a LAAPD if performances found with such a photodetector device are promising.

The size of these different crystals have not been finally decided. Typically, for "small" detectors, the area will be from 25,4 to 51 mm<sup>2</sup> and 51 mm long. We will call "large" crystals a 25,4 to 51 mm<sup>2</sup> area and from 100 to 151 mm long crystal.

The choice of the use of Lanthanum Bromide crystals is based on an improved energy resolution, a fast emission and an excellent temperature and linearity characteristics offered by such material. Typical energy resolution at 662 keV is 3% as compared to Sodium Iodide detectors at 7% and the improved resolution is due to a photoelectron yield of 160% that achieved with Sodium Iodide.

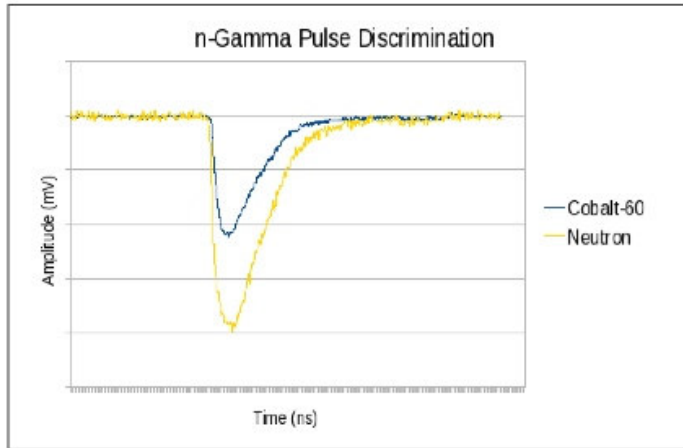


**Fig 1 :** Example of neutron (yellow line) and gamma (blue line) of pulse shape signal coming out from LaBr<sub>3</sub>:Ce crystal

First tests have been concentrated to LaBr<sub>3</sub>:Ce crystal and APD characterization. Some tests have been performed at the York University on the gamma-neutron pulse shape discrimination based on the possible existence of a short and a long light emission components. Using a 1.5"x1.5" LaBr<sub>3</sub>:Ce crystal in coincidence neutron and 4.43 MeV gamma emission from a Am/Be source has been measured. A set of pulse measurement is shown as the figure 1. A full report may be found in the PARIS collaboration website coming to conclusion that such a neutron-gamma discrimination is unsuccessful with a 1.5"x1.5" LaBr<sub>3</sub>:Ce crystal essentially due to La and Br excited state gamma emission after neutron activation.

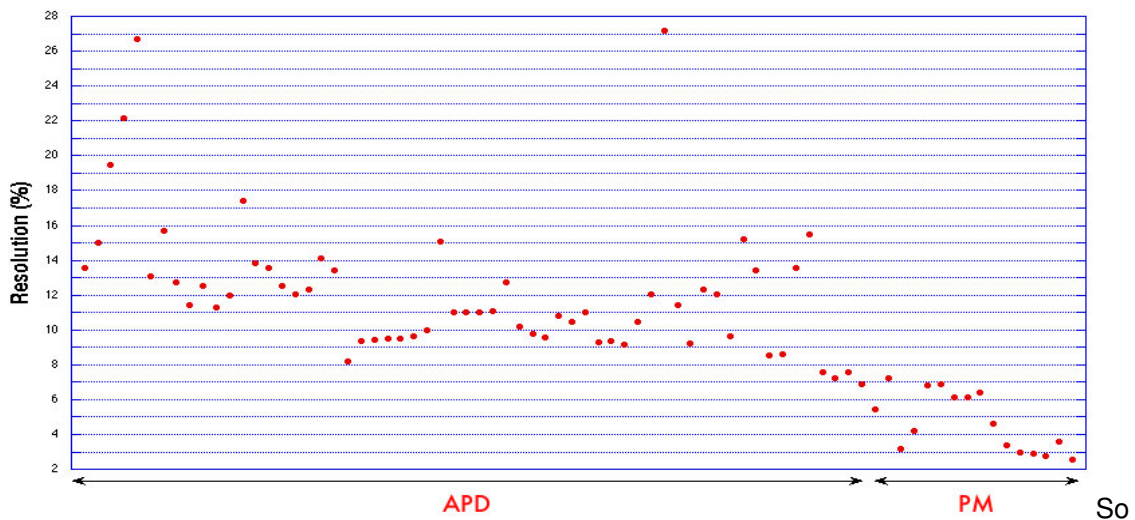


**Fig 2:** Resolution obtained coupling a 1,5"x1,5" LaBr<sub>3</sub>:Ce crystal with an 8664-1010 APD and a PM tube

me developments have been performed at the IPHC-DRS Strasbourg : the construction of a thermostatic box in order to determine the impact with the temperature on the gain, efficiency

and resolution measurement with a 8664-1010 Hamamatsu APD. The stability of the power supply is insured by a high quality Physical Instruments SHQ 222M HV supply. The temperature control is performed within  $\pm 0.1$  °C and an improved linearity of the sensors using a labView interface. Measurement are presently in progress and we would mainly like to answer to question of is it needed to cool down an APD to fulfill our goals. If yes, what would be the best temperature.

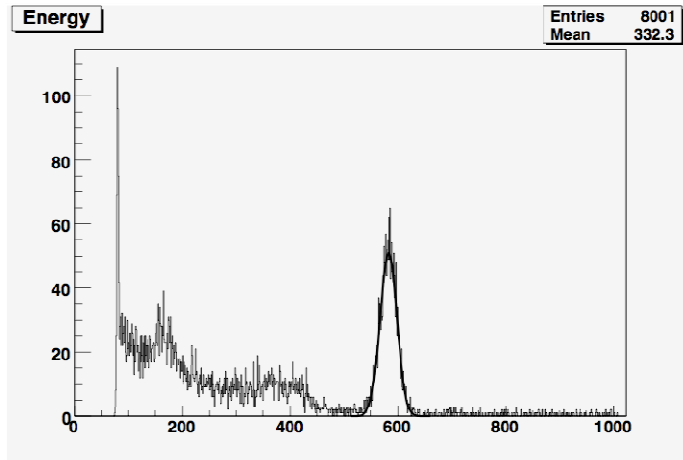


**Fig 3:**  $^{137}\text{Cs}$  spectra obtained the maximum amplitude from pulse shapes

A wide data set have been taken (see fig.2 ) testing the resolution obtained by coupling a 8664-1010 APD with a 1.5"x1.5" LaBr<sub>3</sub>:Ce crystal. We made many tests with different type of preamplifiers (ORTEC 142H, Icare, ...) , different integration constant values, different optical coupling and reflectors (Teflon, guide light in plexiglass, mylar,...) and we finally compare our results with a PM tube. We learnt a lot and finally we found the best resolution of 6.8% obtained at 662 keV using two LAAPDs with teflon reflector at the surface of the crystal, an integration constant of 0.25  $\mu\text{s}$  and an analogical DAQ. We compared our results with a PM tube and finally obtained 2.5% at 662 keV with a 1.2  $\mu\text{s}$  integration constant. Since the surface of the crystal was not fully covered by the APDs, the obtained results are rather encouraging.

We also registered some pulse shapes with a 10 GHz Lecroy oscilloscope. We are now looking for the best algorithm to treat this kind of data. A simple treatment consisting on plotting the maximum amplitude lead already to rather good results as we can see on fig.3.

In a near future, we will test a new preamplifier from M. Ciobanu (FOPI Collaboration - GSI) which has the advantage to get a timing and an energy signal outputs. The first results obtained with à 8664-55 APD were very promising. Since the capacitance of a 8664-1010 APD is much larger, we have to make some tests to validate this preamplifier for the PARIS project.

In addition, a work from the Krakow-Derecen-Sofia-Orsay collaboration (M. Ciemala et al, to be published in NIM) on measurements of high-energy gamma rays with LaBr<sub>3</sub>:Ce detectors has been performed at the 5 MV Van de Graaff accelerator of ATOMKI with (p, $\gamma$ ) reactions such as  $^{27}\text{Al}(p,\gamma)^{28}\text{Si}$ ,  $^7\text{Li}(p,\gamma)^8\text{Be}$ ,  $^{11}\text{B}(p,\gamma)^{12}\text{C}$ ,  $^{39}\text{K}(p,\gamma)^{40}\text{Ca}$  and  $^{23}\text{Na}(p,\gamma)^{24}\text{Mg}$  which lead to a wide gamma-ray energy range from 1368.6 to 17619 keV. The proton beam energy was chosen to lie below neutron threshold. The main results are the curves in fig 4.a and 4.b

showing respectively the LaBr<sub>3</sub> efficiency and internal efficiency as function as the gamma-ray energy.

The plans for year 2009 are the tests of dedicated crystals for PARIS, which were already ordered (by Strasbourg, Kraków, Orsay) from Saint Gobain, using the funds of FP7 SP2PP project and PROVA project. The ordered crystals are of both cubic and cylindrical shape, 2" and 4" long, as well as a phoswich detector (2" long LaBr<sub>3</sub> coupled to 6" long CsI(Na)). This crystals will be coupled to PMT and APDs and tested by using gamma and neutron sources, as well there is a accepted proposal to make a dedicated in-beam test experiment at the Heavy Ion Cyclotron in Warsaw. The ultimate goal is to validate the best option for the PARIS project, choosing between a two separate crystals or a phoswich.

In parallel some light collection simulations will be performed.

A development of a new 500 MHz fast digital electronic card for our project will be work out together with the electronic working group.

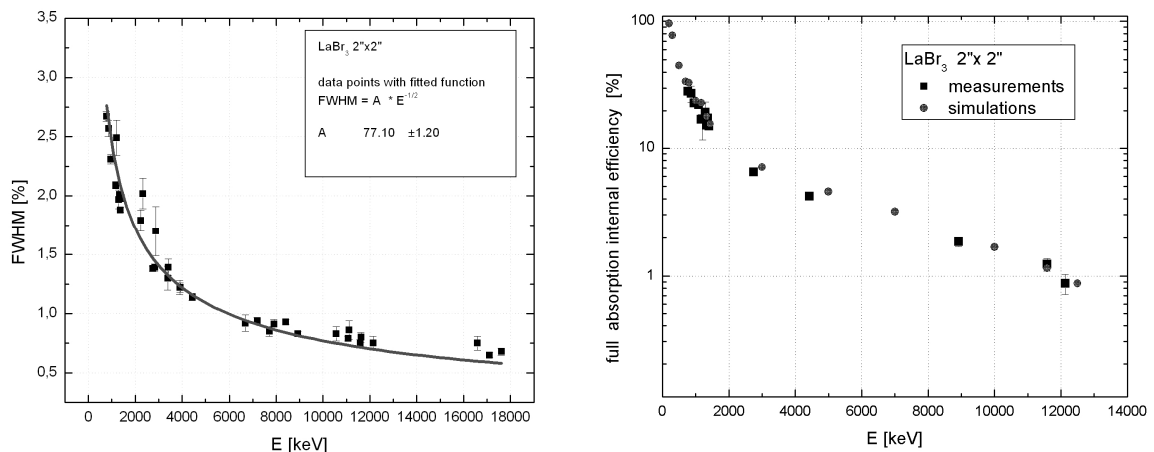


**Fig 4 :** Resolution (left part) and internal efficiency of a 2"x2" LaBr<sub>3</sub>:Ce crystal as function of gamma-ray energy.

## 2.5 Trigger, DAQ, Controls

Digital electronics for reading-out PARIS LaBr3 detector signals are planned to be developed. Digital algorithm optimization or alternatively merging digital and analogue electronics for precise information on the signal timing properties and maintaining in the same time, good energy resolution, is considered. The readout system will be most likely triggerless, synchronized using an external metronome signal (timestamp). Due to many detector channels a design of a dedicated ASICs chips is considered.

The PARIS FEE electronics will be compatible with the GANIL DAQ through the CENTRUM – GAMER- ATOM timestamp distribution system.

The planned R&D in electronics will be based on solutions and competences available from the collaborating groups from: Strasbourg (TNT digital card), Debrecen (miniPET-II module), Milan (analog-digital LaBr3 readout module), Krakow (AGAVA AGATA-VME interface) and GANIL (general overview of the GANIL DAQ)

Basic requirements for the PARIS FEE are the following:

- Serve 200-1000 detector channels (energy and time per channel)
- Deal with fast signals of LaBr3: risetime <1ns, decaytime ~20 ns
- Stand rates up to 100 kHz per a detector channel
- Perform pulse shape analysis for neutron and gamma discrimination and for disentanglement of overlapping signals from phoswich detectors
- Keep time resolution better than 1 ns, for TOF purposes
- Measure energies up to ~50 MeV with 3% resolution.
- Triggerless readout with timestamping
- Provide a gamma time relative to an external signal and gamma energy (or series of energies if from phoswich) with a corresponding timestamp.

## 2.6 Target requirements

*To be defined in the final design report*

## 2.7 Beam requirements

*To be defined in the final design report*

## 3. Implementation and Installation –

*To be defined in the final design report*

### 3.1 Experimental hall and Annex facilities

### 3.2 Detectors-Machine interface

### 3.3 Assembly and installation

## 4. Commissioning (work plan, cost, necessary manpower and other resources)

*To be defined in the final design report*

## 5. Operation (running cost, necessary manpower and other resources)

*To be defined in the final design report*

## 6. Organisations and Responsibilities

### 7.1 Management Board

#### MB

Adam Maj (Krakow) - Project spokesperson

Jean-Pierre Wieleczko (GANIL) – co-spokesperson, GANIL liaison

David Jenkins (York) – co-spokesperson

Jean-Antoine Scarpaci (Orsay) – co-spokesperson

#### Extended MB

O. Stezowski (Lyon), S. Courtine (Strasbourg), O. Dorvaux (Strasbourg), J. Pouthas (Orsay),

P. Bednarczyk (Krakow), C. Schmitt (Lyon), I. Mazumdar (TIFR Mumbai), M. Rousseau

(Strasbourg), F. Azaiez (Orsay)

### 7.2 WBS - work package break down structure

Task Number	Task name	Description of Task	Participating Members (coordinators in bold)
1	Physics cases and theory background	<ul style="list-style-type: none"> <li>Establish pertinent experiments to be run in priority depending on the fundamental issues, on one side, and the installations and detectors available, on the other side.</li> <li>Point out the required experimental resolution and sensitivity for evidencing a given phenomenon.</li> <li>Provide simulations of the reaction kinematics which would define the most suited experimental approach.</li> </ul>	<b>C. Schmitt, I. Mazumdar</b> , F. Azaiez, P. Bednarczyk, S. Courtin, D.R. Chakrabarty, Z. Dombadi, O. Dorvaux, J. Dudek, S. Harisopulos, D. Jenkins, M. Kicinska- Habior, M. Kmiecik, A. Maj, P. Napiorkowski, J.P. Wieleczko, G. Georgiev, D. Balabanski
2	Mechanical design	Develop the PARIS mechanical design for various geometries.	<b>D. Jenkins, S. Courtine</b> , J. Strachan, A. Smith, J. Simpson, S. Kumar
3	Simulations	Test the validity of the 2-shell concept, simulate the performance of the PARIS array for various sizes of the detectors and for various geometries. Find the optimal solution.	<b>O. Stezowski, C.</b> Schmitt, M. Ciemała, M. Chelstowka, A. Maj, M. Kmiecik, O. Roberts, D. Jenkins, S. Courtin, M. Labiche, I. Mazumdar, G.A. Kumar, D.R. Chakrabarty, V. Nanal,
4	Detectors testing	Find out the most appropriate sizes and shapes of the detectors, find out which readout (APD or PMT) shall be the optimal one.	<b>O. Dorvaux, J. Pouthas</b> , Th. Adam, J. Devin, Ch. Finck, C. Mathieu, P. Médina. Ph. Peaupardin, M. Rousseau, J.Schuller, M. Moszynski, M. Ciemała, M. Kmiecik, A. Maj. W. Meczynski, J.P. Wieleczko, O. Roberts, P.Joshi, D.Jenkins, R. Wadsworth, A.Tuff, D. Balabanski, S. Lalkovski, M. Csatos, A. Vitez, A. Krasznahorkay, G. Georgiev, A. Lefebvre- Schuhl, R. Lozeva, J.M. Daugas, S. Erturk

5	Electronics	Decide what front end electronic will be optimal for the PARIS array. Eventually develop the digitisation board.	<b>P. Bednarczyk</b> , J. Pouthas, O. Dorvoux, P. Medina, A. Czermak, B. Dulny, B. Sowicki, M. Zieblinski, P. Joshi, P. Napiorkowski, L. Dimitrov, M. Tripon, P. Doornenbal, S. Pietri, I. Lazarus, Z. Dombradi
6	Synergy with GASPARD (and other detectors)	Find out possible synergies with GASPARD (and other detectors). Propose the common work for PARIS and GASPARD (and other detectors).	<b>J.A. Scarpaci</b> , D. Jenkins, J.P. Wieleczko, A. Maj, M. Labiche, D. Beaumel

### 7.3 Schedule for the signature of Memorandum of Understanding

The PARIS MoU, according to FP7 SP2PP project deliverables, is planned to be signed in 2010.

#### 7. Planning

*Main milestones for the R&D and construction.*

*To be defined in the final design report*

Equipment	End of R&D	Start of construction	End of construction

#### 8. Finances

Cost estimate of the project:

*For each subsystem give a cost evaluation, and the commitment of the different institutions.*

*To be defined in the final design report*

Subsystem	Cost	Expected funds (amount, institution)

*Explain the organisation and work plan that will be established to finance the equipment.*

#### 9. Manpower

*For each task defined in point provide an evaluation of FTE needed for the project, and the commitment of the different institutions.*

*To be defined in the final design report*

Task	Required FTE	Institutions providing the FTE

#### 10. Options and possible further upgrades (list)

*To be defined in the final design report*

## 11. Relations with other projects

### **GASPARD:**

The GASPARD collaboration recently stated that the high energy particles, which detection is needed for certain reactions, need to be measured only in the limited angle ranges:  $5^{\circ}$ - $35^{\circ}$  and  $60^{\circ}$  to  $80^{\circ}$ . For these angles the full energy shall be measured by adding CsI crystals. For the remaining angles Silicon-based telescopes can be used.

GASPARD needs, for some of the physics cases, to measure the sum energy of the whole gamma-rays as well as the single gamma transitions with relatively good resolution in the range up to 5 MeV. For this purpose the PARIS can be used (either whole  $4\pi$  or at backward  $2\pi$ ), without changing the PARIS global design.

This opens very good possibility of synergy between both projects. The PARIS-GASPARD synergy group plans to investigate the influence of GASPARD (detectors, cables, chamber) on the efficiency and resolution of gamma rays, and try to find solutions to minimize this effect.

### **EXOAM2/AGATA:**

PARIS mechanical design and electronics will be compatible with EXOGAM2/AGATA. The work in this aspect is progressing, under the supervision of the Instrumentation Coordination Committee.

### **Other detector systems:**

The possible compatibility with other arrays, as Neutron detector or INDRA/FAZIA, are planned to be worked out.

## 12. Other issues

All remaining issues will be discussed in the forthcoming Technical Proposal